Republic of Iraq
Ministry of Higher Education
And Scientific Research
Al-Nahrain University
College of Science
Department of Physics

Supervised and Unsupervised Classification Performance Satellite Images

A Thesis

Submitted to the College of Science / Al-Nahrain University as a Partial fulfillment

of the requirements of the Degree of Master of Science in Physics

By

Hasan Salim Abed Al-Mageed

B.Sc. 2013

Supervised by

Prof

Dr. Laith A. Al-Ani

Jamadi Al-Thani   *April*

1437 A.H.   *2016 A.D.*

بِسْمِ ٱللَّهِ ٱلرَّحْمَٰنِ ٱلرَّحِيمِ

وَمَآ أُوتِيتُم مِّنَ ٱلْعِلْمِ إِلَّا قَلِيلًا ۝

صَدَقَ اللهُ الْعَلِيُّ الْعَظِيمْ

(سُورَةُ الإِسْرَاءِ:85)

This Humble work is especially dedicated to My Leader and teacher prophet

محمد رسول الله
صلى الله عليه وآله وسلم

Allah messenger (god bless him)

And to the master and the light of my path

Emam Ali bin Musa (peace be upon him)

Spatial dedication to should thank and dedicate this work to my family, my parents, Zahraa, my brothers, and friends.

Also and with much grateful to Dr. Sabih Hamoud Al-Tamimi for his care and follow up and help through my education process.

SUPERVISOR'S CERTIFICATION

I certify that this thesis entitled "**Supervised and Un-Supervised Classification Performance Satellite Images**" was prepared under my supervision at College of Science, Al-Nahrain University as a partial fulfillment of the requirements for the degree of Master of Science in Physics.

Signature:

Name   : Dr. Laith A. AL-Ani

Title   : Professor

Address: Department of Physics

Date   :   /   / 2016

In view of the available recommendations, I forward this thesis for debate by the examination committee.

Signature:

Name   : Dr. Alaa Jabbar Ghazai

Title   : Assistant Professor

Address: Head of Department of Physics

Date   :   /   / 2016

Certification

We certify that we have read this thesis entitled **"Supervised and Unsupervised Classification Performance Satellite Images"** and as examining committee, examined the student (**Hasan Salim Abed Al-Mageed**) in its content and that in our opinion it is adequate with standing as a thesis for the degree of master in science of physics.

Signature: Signature:

Name   : Qais J. Al-Jomaili   Name   : Mohammed S. Mahdi

Title   : Professor   Title   : Assistant Professor

Address: College of science,   Address: College of science, Al-
University of Mustansiriyah   Nahrain University

Date   :   /   / 2016   Date   :   /   / 2016

(Chairman)   *(Member)*

Signature: Signature:

Name   : Alyaa H. Ali   Name   : Dr. Laith A. Al-Ani

Title   : Assistant Professor   Title   : Professor

Address: College of science for woman,   Address : College   of science ,   Al-
University of Baghdad   Al-Nahrain University

Date   :   /   / 2016 (Member)   Date   :   /   / 2016

                                                                (Member and Supervisor)

Approved by the dean of the college of science:

Signature:

Name   : Dr. Hadi M. A. Abood

Title   : Assistant Professor

Address: Dean of science College, Al-Nahrain University

Date   :   /   / 2016

Acknowledgments

First and before all, I present my special thanks for my god for all success that he support and give me through all years of my life which without this support I never could reach this point.

I show my great thanks and respects to my supervisor prof Laith A. Al-Ani for his huge support, guidance and encouragement through my studies, where by his help and instructions I reach to this stage.

Also wont to thanks the physics department and its stuff for help me my study journey

My thanks to the Iraqi Geological Survey authority, for there kind and generous dealing and help in this work.

Abstract

One of the main purposes of remote sensing satellite images is to interpret the observed data and classify features. Satellite image classification plays a major role in the extraction and interpretation of valuable information from massive satellite images.

The primary purpose of this research is to classify multi-spectral Thematic Mapper satellite images using supervised classification. Unsupervised (RGB color model) and supervised classification (maximum likelihood method) is adopted to achieve the classification purpose. The classification accuracy depends upon the selection accuracy of the training area.

PCA Transform is adopted and applied on the original bands to create the principal component images. The first three principle component image contains most the information in all the original bands. For this purpose the first three principle component images are chosen as RGB images to create a colored image.

This colored image has been employed for determining and selecting the training areas which are very important for supervised classification after applying histogram equalization enhancement method on the colored image to make the selection of the training area more clarity and accuracy. After that the selection of the training areas is ready as an input for the supervised classification.

Our results showed that the image with higher variance value doesn't represent a prerequisite in image clarity. The variance with mean value may reflect the quality of the image. The variance and means look like the torque in physics. So that we can see that the image with low variance and mean value near the middle of the dynamic range value has more quality than the image with high variance and mean value near the edge of the minimum or maximum value. Improve the selection of the training area (region of interest) visually plays an essential role in increasing the accuracy of supervised classification and this reflects on the calculation of the area for each class in the scene. In the present work, the overall accuracy increased from 68.5% to 98.9%

after adopting the histogram equalization technique as an enhancement technique in improving the selecting the training area visually.

Although a high classification accuracy with principal component image, but still the classification process with original bands is better because its values represent the real spectral reflectance. The result of classification accuracy with the original bands is enhanced from 68.5% to 97.08% and became very comparable with the result of classification accuracy with the principal component images 98.86% when the selection of the training area (region of interest) has been improved visually.

In this thesis, the ENVI (Environment for Visualizing Images) software version 4.5 has been used to achieve the aim of this study.

List of contents

CHAPTER ONE

General Introduction

1-1   Introduction:

Remote sensing is a science of acquiring information about the earth without actually being in contact with it. This is done by sensing and recording reflected or emitted energy (EMR) and processing, analyzing that information. It functions in harmony with other spatial data-collection techniques or tools of the mapping sciences, including cartography and geographic information systems (GIS) [Jen 07].

Remote sensing makes it possible to collect data on dangerous or inaccessible areas. Remote sensing applications include monitoring deforestation in areas such as the Amazon Basin, the effects of climate change on glaciers and Arctic and Antarctic regions, and depth sounding of coastal and ocean depths [Cla 03].

In remote sensing the emitted energy from the earth's surface is measured using a sensor mounted on an aircraft or spacecraft platform. That measurement is used to construct an image of the landscape beneath the platform. The energy can be reflected sunlight so that the image recorded is, in many ways, similar to the view we would have of the earth's surface from an aero-plane, although the wavelengths used in remote sensing are often outside the range of human vision. As an alternative, the upwelling energy can be from the earth itself acting as a radiator because of its own temperature. Finally, the energy detected could be scattered from the earth as the result of some illumination by an artificial energy source such as a laser or radar carried on the platform. [Joh 13]

The first form of remotely sensed images is "Arial photographs", produced by using camera. Besides the camera, there are another types of remote sensor (e.g. Multi-Spectral Scanner (MSS), Thematic Mapper (TM)). These sensors are mostly carried by satellites (e.g. Land sat-Series, Sea Sat-Series, and spot, etc.) which are scanning the earth's surface daily. Therefore, a satellite or airborne multi-spectral sensor provides data in the form of several spectral images of the particular area of the earth under observation. Each image represents the spatial distribution of reflected or emitted electromagnetic energy as seen through a given spectral window or band [Lai 96].

In the last decades, satellite images became the main sources of information because they can also be utilized for different applications such as agricultural, desertification, monitoring land cover change, monitoring urban growth, forestry, hazards, natural disasters, oceanography, water resources, observing settlement expansion, and so on. Remotely sensed data is a very essential application in land use planning and management. It is a helpful tool for land use/ land cover identification and classification of various features of the land surface in an image received from satellite [Muk 13]. It provides a reliable information about the characteristics of various land areas and their behavior under different land uses. Land use planning has become more and more important for local authorities to better manage the environmental resources and get closer to sustainable conditions. However, there is a need to evaluate the techniques locally in terms of effectiveness and simplicity [Muk 13].

The technique of Principal Component Analysis (PCA) has found wide use in digital processing of multispectral satellite images. PCA and image fusion techniques are often used to enhance an image particularly in the land-cover classification of satellite images, where such images are used for increasing the interpretability of human observers and for improving the accuracy of the classification. In the field of remote sensing, especially in hyper spectral imagery, reduction of the dimensionality is a key point for data analysis to prevent from Hughes phenomenon. A novel image fusion scheme is proposed for multispectral and panchromatic satellite images using Principal Component Analysis (PCA) and Non sub Sampled Contour let Transform (NSCT) [Hai 10]. Numerous satellites collect correlated data from earth surface with different spatial, spectral and temporal resolutions. Given the design constraints sensors with high spectral resolution, do not have an optimal spatial resolution, and vice versa. For optimal use of these data the fusion of multispectral and panchromatic images is becoming a promising technique to obtain images with high spatial and spectral resolution simultaneously. [Dav 15]

1-2   Resolution of Remote Sensing

The Resolution (or resolving power) is a measure of the ability of an optical system to distinguish between signals that are spatially near or spectrally similar [Jen 86, Swa 78].
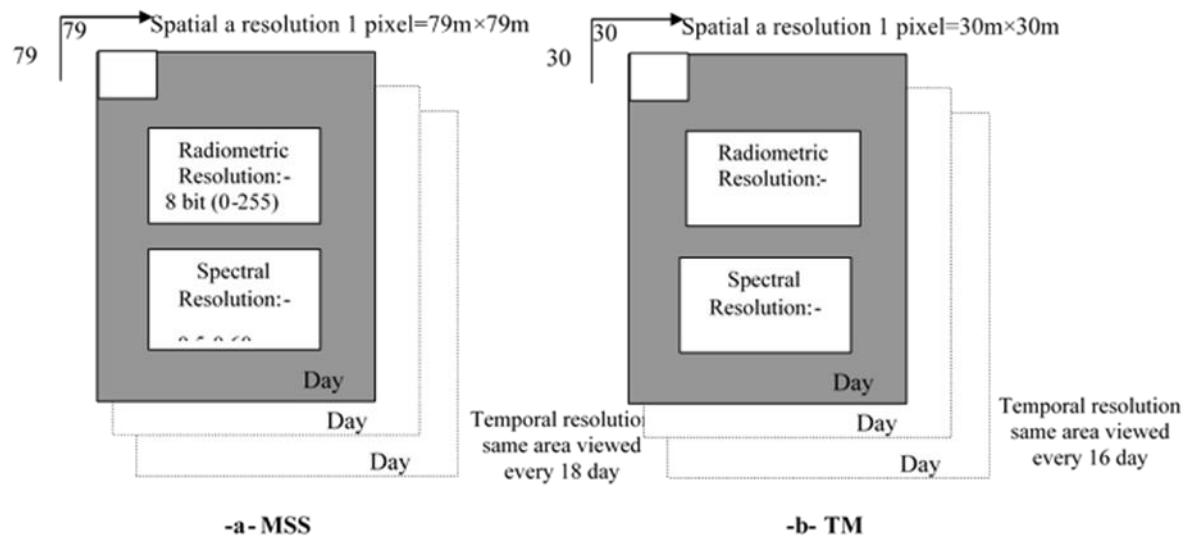

Figure (1-1) a- Landsat (MSS) – band 4, b- Landsat (TM) – band 1 (Four types of Resolution)

In remote sensing we can consider four types of resolution, i.e. Spectral, Temporal, Radiometric and Spatial. Figure (1-1) illustrates all these types of resolutions, and could be defined as follows [Ema 01].

a) Spectral Resolution

Spectral resolution represents the spectral band width of the filter and the sensitiveness of the detector. The spectral resolution may be defined as the ability of a sensor to define fine wavelength intervals or the ability of a sensor to resolve the energy received in a spectral bandwidth to characterize different constituents of earth surface. The finer the spectral resolution, the narrower the wavelength range for a particular channel or band. Many remote sensing systems are multi-spectral, that record energy over separate wavelength ranges at various spectral resolutions. For example IRS LISS-III uses 4 bands: 0.52-0.59 (green), 0.62-0.68 (red), 0.77-0.86 (near IR) and 1.55-1.70 (mid-IR). The Aqua/Terra MODIS instruments use 36 spectral bands, including three in the visible spectrum. Recent development is the

hyper-spectral sensors, which detect hundreds of very narrow spectral bands [Gib 00]. Figure (1-2) shows the hypothetical representation of remote sensing systems with different spectral resolution.
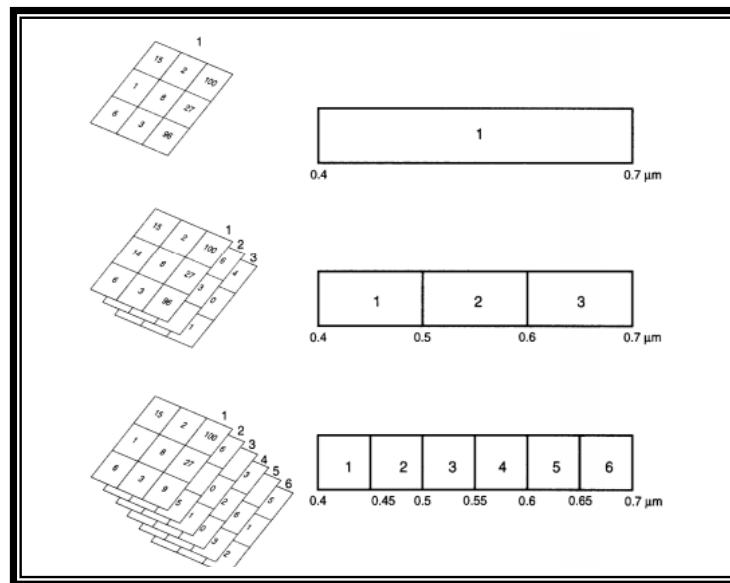

Figure (1-2) Examples of remote sensing systems with different spectral resolution [Gib 00]

The first representation shows the DN values obtained over 9 pixels using imagery captured in a single band. Similarly, the second and third representations depict the DN values obtained in 3 and 6 bands using the respective sensors. Landsat (MSS) obtains data in four bands, and each pixel consequently has four digital numbers associated with it, whereas the Landsat (TM) system is a seven-band system. Thus Landsat (TM) has a better spectral resolution than Landsat (MSS) [Gib 00].

b) Temporal Resolution:

The temporal resolution of a remote sensing system is a measure of how often data are obtained for the same area. Landsat 5, for example, has a repeat cycle of 16 days, and Landsat 1, 2, and 3, has a repeat cycle of 18 days [Gib 00].

c) Radiometric Resolution:

The radiometric resolution of a remote sensing system is a measure of how many gray levels are measured between pure black and pure white [Gib 00]. The number of gray levels can be represented by a greyscale image is equal to (2^n), where

n is the number of bits in each pixel [Tar 10]. Frequently the radiometric resolution is expressed in terms of the number of binary digits, or bits necessary to represent the range of available brightness values [Joh 13, Tar 10]. The maximum number of brightness levels available depends on the number of bits used in representing the energy recorded. Thus, if a sensor used 8 bits to record the data, there would be ($2^8 =$ 256) digital values available, ranging from 0 to 255

d) Spatial Resolution:

A measure of the amount of detail that can be observed on an image [Gibson: 00], or is a measure of the smallest angular or linear separation between two objects that can be resolved by the sensor [Jen 86].

1-3   Thematic Mapper (TM):

The Thematic mapper is a remote sensor with seven spectral bands covering the visible, near infrared and thermal (far) infrared regions of the spectrum, this sensor was carried by Landsat 4 and 5 [Hor 85].

(TM) sensor on Landsat 4 and 5 recorded data in 8 bit (i.e. $2^8 = 256$) gray levels in 7 wavebands from (0-255) [Swa 78]. The satellite orbits the earth once every 99 min, resulting in 14.5 orbits per a day rotation of the earth shifts the orbital path each day so that at the end of 16 days or 233 orbits (flight path) [Sab 78], most of the land and sea surfaces of the earth are covered between altitude (row) 82° north and 82° south's. Four detector arrays were used for IR bands, while the other bands use 16 detectors [Ban 97].

The satellite orbits are also near polar but they are at a lower altitude then the previous series approximately 705km [Hor 85] It obtains data in seven wave bands with a (30m$\times$ 30m) resolution in bands 1 to 5 and 7 (for all bands except the thermal band 6) and (120m$\times$ 120m) resolution in band 6 [Ban 97]. The main features of the Thematic Mapper (TM) Landsat shown in Table (1-1)

Table (1-1) Land sat 4 and 5 – Thematic Mapper(TM) sensor [Hor 85]

Band	Color	Spectral (μm)	Spatial (m)	Temporal	Sensitivity [Radio-metric resolution]
1	Blue	0.45-0.52	30× 30	16 days	0.8%
2	Green	0.52-0.60	30× 30	16 days	0.5%
3	Red	0.63-0.69	30× 30	16 days	0.5%
4	Near-IR	0.76-0.90	30× 30	16 days	0.5%
5	Mid-IR	1.55-1.75	30× 30	16 days	1.0%
6	Thermal IR	10.4-12.5	120×120	16 days	$0.5k^{0}$ NETD
7	Far-IR	2.08-2.35	30× 30	16 days	2.4%

1-3.1 Characteristics of (TM) Spectral Bands:

a. **Band 1:** (0.45-0.52) μm - (visible part), blue. This band provides increased penetration into water bodies as well as supporting analysis of land use soil, and Vegetation characteristics, also useful for soil/vegetation discrimination, forest type mapping and cultural feature identification [Afa 96, Hor 85].

b. **Band 2:** (0.52-0.60) μm - (visible part), green (green reflectance by healthy vegetation). This band provides useful information in many agriculture applications designed to measure green reflectance peak of vegetation, it is an important band for detecting green vegetation.

c. **Band 3:** (0.63-0.69) μm - (visible part), Red. This band provides very high contrast in many scenes and therefore it is one of the best bands for soil boundary and geological boundary delineation because of the reduced effect of atmospheric attenuation. This is a red chlorophyll absorption band of healthy green vegetation; it is an important vegetation discriminator [Lli 00].This band between (0.6-0.68) provides good appearance of water bodies [Ahm 97]. The (0.69) cut off is significant because it represents the beginning of a spectral region from (0.68) to (0.75) , where vegetation reflectance cross over take place that can reduce the accuracy of vegetation studies [Lai 96].

d. Band 4: (0.76-0.90) *μm* - (near or reflective infrared part). This band is especially responsive to the amount of vegetation biomass present in a scene. It is useful for crop identification; emphasize soil-crop and land –water contrast [Hord: 85].

e. Band 5: (1.55-1.75) *μm* - (mid infrared part). This band is sensitive to the amount of water in plants; it is one of the few bands that can be used to discriminate between clouds snow and ice, so important in meteorological hydrologic research, indicative of vegetation moisture content, soil moisture and differentiation of snow from clouds [Ban: 97].

f. Band 6: (10.4-12.5) *μm* - (thermal far IR). It is useful for locating geothermal activity, thermal inertia mapping for geologic studies, vegetation classification, vegetation stress analysis, and soil moisture studies and thermal mapping applications. This band measures the amount of IR radiant flux emitted from surface [Lai 96].

g. Band 7: (2.08-2.35) *μm* - (far IR). It is an important band for the discrimination between geologic rock formations useful for discrimination of mineral and rock types, also sensitive to vegetation moisture content [Lli 00]. It has been shown to be particularly effective in identifying zones of hydrothermal alteration in rocks [Hor 85].

1-4   Spectral Reflectance Curves:

Spectral reflectance curves or spectra are usually determined by instruments, which record the observed energy, called spectrometers [Jen 86].

The spectrometer is basic component in a number of instruments used in spectral analysis [Swa 78].

Interaction of electromagnetic radiation (EMR) with earth's surface can be presented by reflection, absorption, or transmission; of the incident radiation [Wafaa: 99]. Sun light reflected from materials is measured as a function of wavelength, the effective utilization of remote sensor data requires knowledge and understanding of:-

   1- Spectral characteristic of various earth surfaces.

2- The factors that influence the spectral characteristics.

One may derive information about the materials covering the surface of earth from the spatial and spectral distributions of energy emitted from those materials; the temporal (time) variations in the scene are also useful in the information's extraction process [Lai 96].

Figure (1-3) shows typical spectral reflectance curves for different characteristic types of earth surface materials [Sie, Men 05].
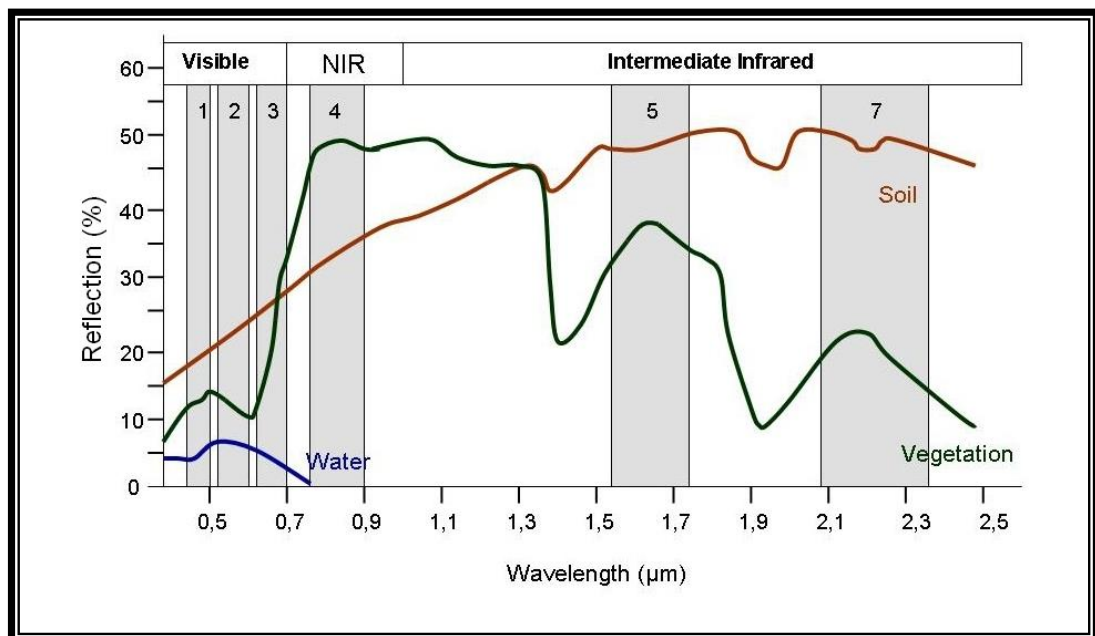

Figure (1-3) Spectral signatures of soil, vegetation and water source: (Sie, Men 05) with modifications

Most satellite-based passive remote sensing systems obtain data in the visible and infrared and a knowledge of the reflectance characteristics of vegetation, soils, water, rocks and urban.

1-5   Principal Components Analysis (PCA):

Principal Components Analysis (PCA) is a linear transformation technique related to Factor Analysis. Given a set of image bands, PCA produces a new set of images, known as components, which are uncorrelated with one another and are ordered in terms of the amount of variance they explain from the original band set. PCA has traditionally been used in remote sensing as a means of data compaction.

For a typical multispectral image band set, it is common to find that the first two or three components are able to explain virtually all of the original variability in reflectance values. Later components thus tend to be dominated by noise effects. By rejecting these later components, the volume of data is reduced with no appreciable loss of information. Given that the later components are dominated by noise, it is also possible to use PCA as a noise removal technique. The output from the PCA module includes the coefficients of both the forward and backward transformations. By zeroing out the coefficients of the noise components in the reverse transformation, a new version of the original bands can be produced with these noise elements removed. Recently, PCA has also been shown to have special application in environmental monitoring. In cases where multispectral images are available for two dates, the bands from both images are submitted to a PCA as if they all came from the same image. In these cases, changes between the two dates tend to emerge in the later components. More dramatically, if a time series of band images (or a similar single-band index) is submitted to the analysis, a very detailed analysis of environmental changes and trends can be achieved. In this case, the first component will show the typical band over the entire series while each successive component illustrates change events in an ordered sequence of importance. By examining these images, along with graphs of their correlation with the individual bands in the original series, important insights can be gained into the nature of changes and trends over the time series [Jen 04].

1-6   Image Enhancement:

Image enhancement is concerned with the modification of images to make them more suited to the capabilities of human vision. Regardless of the extent of digital intervention, visual analysis invariably plays a very strong role in all aspects of remote sensing. While the range of image enhancement techniques is broad, the following fundamental issues form the backbone of this area:

1. Satellite-based scanner imagery contains a variety of inherent geometric problems such as skew (caused by rotation of the earth underneath the satellite as it

is in the process of scanning a complete image) and scanner distortion (caused by the fact that the Instantaneous Field Of View (IFOV) covers more territory at the ends of scan lines, where the angle of view is very oblique, than in the middle). With commercially-marketed satellite imagery, such as LANDSAT, IRS and SPOT, most elements of systematic geometric restoration associated with image capture are corrected by the distributors of the imagery. Thus, for the end user, the only geometric operation that typically needs to be undertaken is a rubber-sheet resampling in order to rectify the image to a map base. Many commercial distributors will perform this rectification for an additional fee [Eas 01].

2. Photogrammetry is the science of taking spatial measurements from aerial photographs. In order to provide a full rectification, it is necessary to have stereoscopic images—photographs which overlap enough (e.g., 60% in the along-track direction and 10% between flight lines) to provide two independent images of each part of the landscape. Using these stereoscopic pairs and ground control points of known position and height, it is possible to fully recreate the geometry of the viewing conditions, and thereby not only rectify measurements from such images, but also derive measurements of terrain height. The rectified photographs are called orthophotos. The height measurements may be used to produce digital elevation models. Contrast Stretch Digital sensors have a wide range of output values to accommodate the strongly varying reflectance values that can be found in different environments. However, in any single environment, it is often the case that only a narrow range of values will occur over most areas. Grey level distributions thus tend to be much skewed. Contrast manipulation procedures are thus essential to most visual analyses. Figure (1 - 4) shows TM Band 3 (visible red) and its histogram. Note that the values of the image are quite skewed. The right image of the figure shows the same image band after a linear stretch has been applied. This is normally used for visual analysis only—original data values are used in numeric analyses [Eas 01].
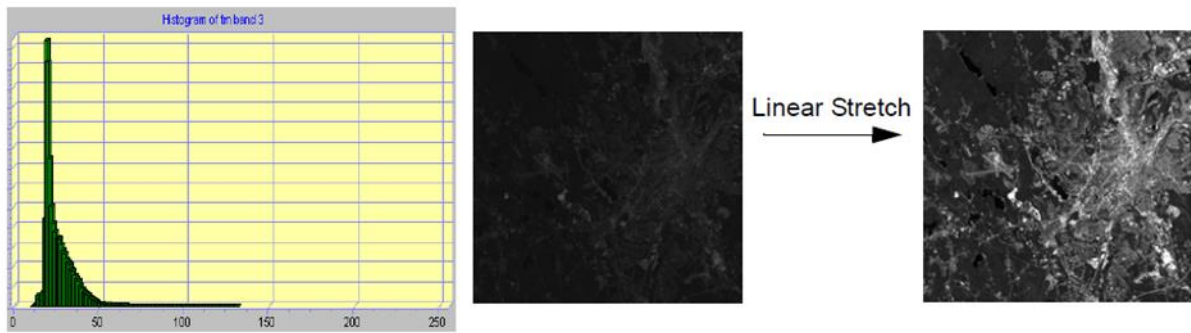
Figure (1 - 4) TM Band 3 and its histogram and the result of TM band after applying linear stretch

1-7   Composite Generation:

For visual analysis, color composites make fullest use of the capabilities of the human eye. Depending upon the graphics system in use, composite generation ranges from simply selecting the bands to use, to more involved procedures of band combination and associated contrast stretch. Figure (1 - 5) shows several composites made with different band combinations from the same set of TM images [Eas 01].
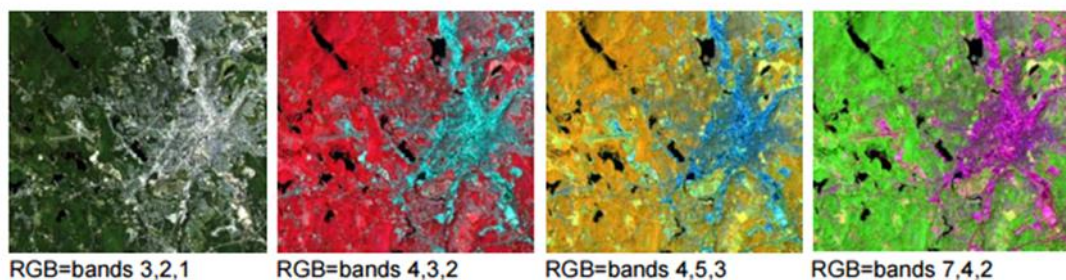

RGB=bands 3,2,1   RGB=bands 4,3,2   RGB=bands 4,5,3   RGB=bands 7,4,2

Figure (1 - 5) several composites made with different band combinations from the same set of TM images

1-8   Image Classification:

One of the main purposes of remote sensing satellite images is to interpret the observed data and classify features. Satellite image classification plays a major role in extract and interpretation of valuable information from massive satellite images. The satellite image classification is a very important problem in the geographic studies, because using these methods are possible to determine that ground classes or

uses exist in a certain zone of study, because a satellite image has colors, shapes and forms that determine this uses. [Lai 96]

The overall objective of image classification procedures is to automatically categorize all pixels in an image into land cover classes or themes. Normally, multispectral data are used to perform the classification and the spectral pattern present within the data for each pixel is used as the numerical basis for categorization. Classification techniques can be grouped into supervised and unsupervised [Bla 10]:-

1-8-1   Supervised classification:

Supervised classification uses a priori information inferred from examples, supposing to know to which class they belong, without any a priori definition of similarity. It is a result of an iterative procedure, which tries to find a mathematical formalism to reproduce the expert's way of assigning class memberships to patterns. The iterative process is often referred to as training or learning phase of the classifier. Besides this, parameters governing operational characteristics of the classifiers have to be identified by trial and error or by optimization procedures. Once trained, the classifier is then used to attach labels to all the image pixels according to the trained parameters [Dav 15].

1-8-2   Unsupervised classification:

In unsupervised methods, the characteristics of the classes are unknown, so the classification algorithm explores the image and compute clusters that represent groups of pixels with similar spectral properties. Therefore, unsupervised classification is based on a suitable definition of similarity between patterns rather than on a priori knowledge of their class membership. The task of unsupervised classification can be formulated as finding groups with a minimum degree of heterogeneity, being most distant from each other. The degree of heterogeneity is defined as a distance measure, such as the Euclidean distance, the Mahalanobis distance or the adaptive determinant criterion [Dav 15].

1-9 Historical Review:

Principal Component Analysis (PCA) is an important data transformation technique used in remote sensing work with multi-spectral and multi-temporal data, and it is one of the oldest techniques that are used in multivariate analysis.

The technique of PCA was first described by Karl person in 1901, he believed that this was correct solution to some of the problems that were of interest at that time [Aly 98]. Hotelling then developed it in 1933. Therefore, Hotelling was the first who derive and publish the transformation that transform discrete variables into uncorrelated coefficients, he referred to this technique as the method of PC's [Gon 87].The transformation use for transforming correlated data into a set of uncorrelated coefficients was discovered by Karhunen and Loeve. In 1947, Karhunen used this transform in setting of the probability theory and subsequently generalized with Loeve in 1948 Therefore, this transform called Karhunen-Loeve transformation [Aly 98].

In 1962, Simonds reviewed the philosophy of the characteristic vector analysis to promote increased understanding and utilization of the method. The results show that the characteristic vector analysis of multivariate response data successfully applied to a variety of optical and photographic response function [Sim 62].

In 1973, Patrick applied the Karhunen-Loeve transformation on a multi-spectral data for information extraction. This transform provide a set of uncorrelated principal component images which are very useful in automatic classification and human interpretation [Rea 73].

In 1979-1980, Byrne stated that the PC is direct outcome of the high correlation that exists between dates for regions that are relatively constant and the low correlation associated with the region that are quite different with time [Byr 80].

In 1978, Santisteban studied the principal components of multi-spectral image with special emphasis placed on photo interpretation application. The results have been particularized to land-sat multi-spectral scanner images and applied to the geological study of a sedimentary basin in central Spain [San 78].

In 1985, Ashbindu applied standardized and un-standardized principal component on a land sat MSS sub scene. The results indicate substantial improvement in S/N ratio and image enhancement by using standardized variables in the principal component analysis [Sin 85].

In 1985, Anita presented automatic method for segmentation of metrological satellite data using a multi-dimensional clustering procedure. The data transformed before segmentation by use of the principal component transformation [Sed 85].

In 1989, Chavez applied selective PCA for extracting spectral contrast in Land sat TM mapper image data. The result shows that selective PCA can be used to enhance and map the spectral differences or contrast between different spectral regions [Cha 89].

In 1994, Douglas evaluated four change detection techniques using multi-spectral multi-temporal SPOT data for identifying changes in hardwood forest defoliation. The change detection techniques were PCA, image differencing, temporal change classification, and post classification change differencing. The result indicates that the defoliation best determined by PCA and image differencing [Muc 94].

In 1994, Xiuping J. and John A. R. research for the efficiency of the maximum likelihood method, as a result they reach that the original data used without transformation, the modified function has the same form as the conventional maximum likelihood function. The ML method simply achieve a feasibility and a high relative accuracy in the classification process [Xiu 94].

In 1996, Laith applied principal component analysis on six TM satellite images for enhancement and color image composition. The researcher applied maximum likelihood method to classify the TM satellite images. The results show that the overall classification accuracy is 83% [Lai 96].

In 1999, Wafaa applied maximum likelihood and minimum distance method for classifying digital TM satellite images. The results show that the classification accuracy improved with maximum likelihood approach [Waf 99].

In 1999, Miriam implemented K-means clustering in both software and re-configurable hardware. The overview of the K-mean algorithms and some of the decisions made for an implementation also presented [Lee 99].

In 2001, Arjen applied two approaches taken to manage large data sets, principal component analysis and cluster analysis [Arj 01].

In 2001, Lorenzo and Diego used the maximum likelihood method as unsupervised classification, were they proposed a technique of classify the satellite image without taken any reliable ground training area for the classification, were the method depend on the unsupervised concept for classify the scene [Lor 01].

In 2007, Wei and Qihao made a survey of the accuracy and the effectiveness of the supervised and unsupervised classification methods where they reach that the classification affected by many factors as the quality of the imagery and the design of the classification procedure. It is difficult to identify the best classifier but it has been notice that the combination of different classification approaches are helpful for improvement of classification accuracy [Wei 07].

In 2009, Al-Ahmadi and Hames has operated four classification methods ISODATA (unsupervised) and minimum distance, maximum likelihood and Mahalanobis distance methods (supervised) on a set of remote sensing data, as a result the maximum likelihood show the best accuracy in the classification, but in the same time the both Minimum distance and Mahalanobis distance methods overestimated agriculture land and suburban areas [Al-Ahm 09].

In 2010, Perumal and Bhaskaran made a comparison between the supervised and the unsupervised classification method to classify remote sensing data with high spatiotemporal dimensions, as a result they been reach that the Mahalanobis classifier shows a high accurate result and a simple method simultaneously, and the important of the right chose of the classification method depending on the selected set of data [Per 10].

In 2011, Laith and Mohammed used the PCA transformation method to classify the satellite images, where as a result that the PCA transformation method

give a relatively good classification accuracy percentage, and can be used as a method for image classification [Lai 11].

In 2011, Gil, Yu, Lobo, Lourenço, Silva and Calado has used different supervised classification methods on the image that been taken with the High Spatial Resolution IKONOS for make a vegetation mapping, as a result of the use of this different methods they clarify that the use of the maximum likelihood method yields to a high accuracy per class and that improve the classification by increase the quantity and the quality of the training area [Gil 11].

In 2012, Asmala used the maximum likelihood classification on the multispectral bands. Where the ML classified the study area into 11 classes, with accuracy 97%. ML classifies pixels based on known properties of each cover type [Asm 12].

In 2012, Subhash, Akhilesh and Seema used the supervised methods for classification. They reach a result that the maximum likelihood method (overall efficiency 84%) is more applicable and reliable for the satellite image classification purposes. While the Mahalanobis method has given more reliable results than the Minimum distance method [Sub 12].

In 2013, Laith has found out a generic method (Ant Colony system) used to classify conceptual multiband imagery, where the ACO has used to found out the optimal number of classes that may exist in the imagery. It has been found that the classification result by ACO are in a good agreement with the actual training data [Lai 13]

In 2013, Kanika, Anil and Rhythm compared and analyzed all the techniques for best results and maximum accuracy, According to the results it stated that among all the supervised algorithms discussed generally K-Nearest Neighbor provides good results as compared to other algorithms in terms of accuracy but it has high time complexity [Kan 13].

In 2013, Christopher, Segun and Inemesit considers the effectiveness of some Supervised Learning Methods in the Mapping of Built up Areas from Landsat-based

Satellite Imagery, they tested the supervised method on the urban area where it proved the best classifier with a total extracted ISA followed by Support Vector Machine and Minimum distance classifier [Chr 13].

In 2013, Carlos, Erivelto, Victor, and Diego studied the evaluation of the supervised classification method, were they show that each classifier has advantage in some stages and disadvantage in another, they show that maximum likelihood method perform has very high response in producer's accuracy while in the user's it shows a low accuracy [Car 13].

In 2013, Manoj, Astha, Potdar, Kalubarme and Bijendra made a compression between unsupervised classification methods as a result they shows that each various classification techniques for satellite images shows a different accuracy. Hybrid method of SRG and Mahalanobis technique leads to better accuracy [Man 2013].

In 2013, Balaji and Sumathi by using the k-mean classification method shows that it is possible to reduce the computational cost avoiding feature calculation for every pixel in the image [Bal 13].

In 2014, Parivallal used the supervised classification methods to classify the google maps images, where he compered between methods and analyzed the result so he shows the problems that face each method according to the accuracy for each method [Par 14].

In 2014, Priyanka, Khobragade and Tehre used the supervised method in order to identify the land use by the crops, were defined the useful of the classification that appear the placed of the growing crops [Pri 14].

In 2014, Sabna and Ratika used the supervised and unsupervised methods to shows the image classification as one way of mapping land use and land cover. They tested the method and has been shown that they are useful to describe the images and turn them to a useful map [Sab 14].

In 2014, Maryam, Vahid and Mehdi used the supervised maximum likelihood classification method to classify the Bivareh forests. As results showed that support

vector machine (SVM) with Kappa coefficient 0.7069 and overall accuracy 88.65% is more accurate than other methods [Mar 14].

In 2015, Sunitha and Suresh studied the satellite image classification methods and techniques, and also compared various satellite image classification methods. Were they shows the major advantage and dis advantage of the classification requirements and efficient [Sun 15].

In 2015, Thwe, Aung and Hla used the unsupervised clustering method to classify Satellite image (Mandalay area in 2001). After clustering. They defined a specific range of three clustered were they chosen this ranges to obtain the Greenland, water and urban balance [Thw 15].

In 2015, Harikrishnan compare the analysis of supervised and unsupervised algorithm for satellite image classification, and he studied the accuracy assessment for each algorithm is studied and analyzed it. He obtained that by using obtained output image one can able drawn solution for certain problem in particular region [Har 15].

In 2015, Yulin, Xiaowei, Yun, Hiroyuki, Koki and Ryosuke S., considered an approach which is able to automatically select training samples from satellite images by propagating common knowledge through the unlabeled data[Yul 15].

1-10 Aim Of Thesis:

The primary purpose of this research is to classify multi-spectral Thematic Mapper satellite images using supervised classification. Unsupervised and supervised classification is adopted to achieve the classification purpose. The maximum likelihood (supervised classification method) classifier is generally considered to be the most powerful but is also considered the most computer intensive. According to this Maximum likelihood algorithm is adopted to achieve this purpose

One of the most important concept of pattern recognition in remote sensing is the definition of the classes in to which the data to be categorized. The accuracy of a

supervised classification analysis will depend up on the selection accuracy of the training area.

PCA Transform is applied on the original bands to create the principal component images. The first three principle component images are chosen as RGB images to create colored image (Unsupervised classification method).

This colored image is adopted for determining the training area which are very important for supervised classification after applying histogram equalization enhancement method on the colored image to make the selection of the training area more clarity and accurate.

1-11 Thesis Organization:

This thesis consists of four chapters:-

Chapter one dedicated for general introduction with a historical review for the principal component and Image classification techniques.

Chapter two describes the theoretical concepts, for all methods and techniques applied tin the present.

Chapter three demonstrates and discuss the obtained results for all the methods applied in the present work.

Chapter four include the conclusion of the results and the proposed future work.

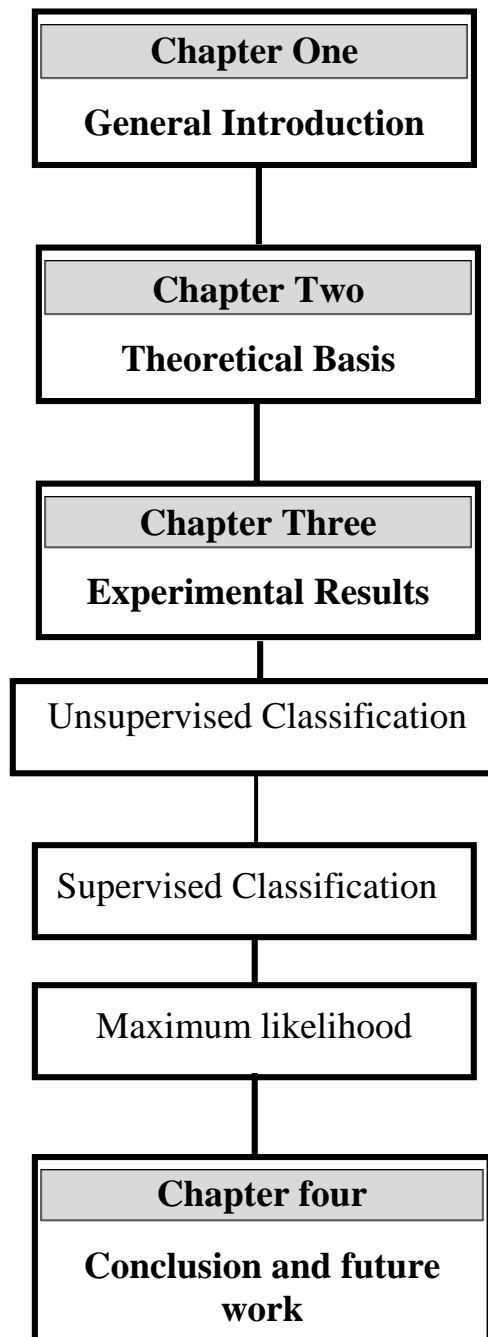The overall scheme of general work in our thesis, can be summarized in figure (1-7).

Chapter One

General Introduction

Chapter Two

Theoretical Basis

Chapter Three

Experimental Results

Unsupervised Classification

Supervised Classification

Maximum likelihood

Chapter four

Conclusion and future work

Fig (1-7) Block diagram describing the contents of the thesis

CHAPTER TWO

Theoretical Basis

2-1 Introduction:

The information that the remote sensed image provides can be very helpful in many particular human usage, (as civilian or military uses). But, to deal and use this information, the imagery must be go through some process, where by applying this process will extract and modify the information to it can become clear, and handily to use.

The image processing is a vital stage for identifying and clarify the remote sensed image, this stage composed of Image transformation, Image enhancement and Image classification.

This chapter demonstrates with the theoretical basis for all techniques that can be adopted and applied in this research starting from the image enhancement technique like coloring, histogram equalization and principal component analysis reaching to the maximum likelihood method as supervised classification method which is the main purpose of this research.

2-2 Image Transformation:

The multispectral or vector character of most remote sensing image data renders it an enable to spectral transformations that generate new sets of image components or bands. These components then represent an alternative description of the data, in which the new components of a pixel vector are related to its old brightness values in the original set of spectral bands via a linear operation. The transformed image may make evident features not discernible in the original data or alternatively it might be possible to preserve the essential information content of the image (for a given application) with a reduced number of the transformed dimensions. The last point has significance for displaying data in the three dimensions available on a color monitor or in color hardcopy, and for transmission and storage of data.

Transformation theory has played an important key role in most signal and image processing. One of the most important transform that has been so far used, and will be considered in this chapter is the principal component analysis (PCA). Analogous transformation for transforming continuous data into a set of uncorrelated

coefficients is called the (KLT) Karhunnen –Loeve expansion [Laith: 96]. The (PCs) transformation (also referred to as the eigenvector transformation) also called Hotelling transformation [Sim 62]. Hotelling in 1933 [Hot 33] who was the first derived and published this transformation to transform discrete variables into uncorrelated coefficients. [Lai 96, Sin 85]. Figure (2-1) shows the correlation property of the data in raw feature space and the data in PC'S space.
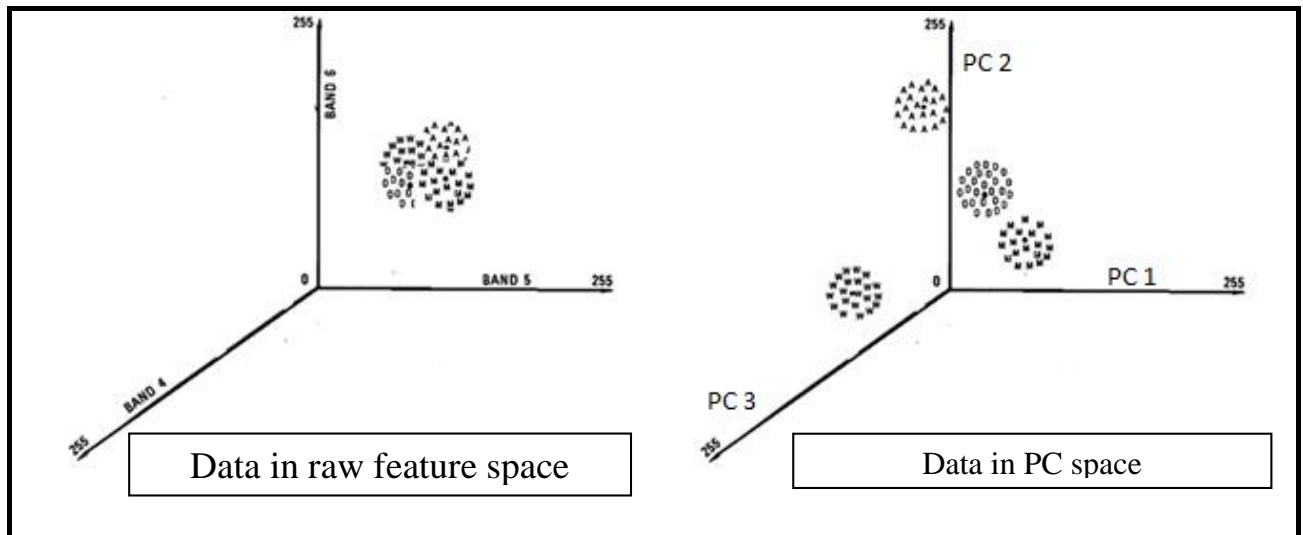

Figure (2-1) De-correlation property in PC feature space [Ema 00].

The KL-transformation is a method of information compression, feature extraction and rotation applications. [Gon 87] The aim of such transformation is to generate new, decorrelated images from partially statistically correlated images [Sim 62]. It has been found that PC expansion minimizes the mean square error [Ema 01].

2-2-1   Principal Component Analysis:

The principal component analysis is based on the fact that neighboring bands of hyper spectral images are highly correlated and often convey almost the same information about the object. The analysis is used to transform the original data so to remove the correlation among the bands. In the process, the optimum linear combination of the original bands accounting for the variation of pixel values in an image is identified.

The PCA employs the statistic properties of hyper spectral bands to examine band dependency or correlation. Though, one may find many synonyms for PCA, such as the Hotelling transformation or Karhunen-Loeve transformation [Gon and

Woo 08]. All these transformations are based on the same mathematical principle known as eigenvalue decomposition of the covariance matrix of the hyper spectral image bands to be analyzed.

The PCA is commonly used technique for remote sensing image analysis, it has been used for determining the underlying dimensions of remotely sensed data, data enhancement for geological applications and land-cover change detection [Fun 87].

The purpose of PCA is to define the number of dimensions that are present in a data set and to fix the coefficients, which specify the positions of that set of axes, which point in the directions of greatest variability in the data [Lai 96].

Therefore, the PCA is a mathematical transform that produces new images based on the variance of the multi-spectral data set. This is one of the most popular transformations applied to multi-spectral data produces a series of linear transformations of the observed variables that result in a new. The principal uses of this transformation are in data compression and rotation applications [Aly 98].

This technique used to produce de-correlated images from correlated images is order to reduce the dimensionality of a set of responses to an intrinsic minimum.

In our work, the PCA is adopted to perform image region classification and image data compression and PCA has several advantages and disadvantage which can be summarized by the following points.

2-2-1-1 Advantages and disadvantages:

The PCA which reduces the number of characters by finding two or three new characters that are combinations of the old characters.

- **The PCA has several advantages:- [Aly 98]**

  a. Most of the variance in a multi-spectral data set is compressed. The information contents of a number of band imagery for example (seven TM bands) in to just two or three transformed PC images. The transformation provides uncorrelated variables with the first two or three components

generally containing (90 % – 97 %) of the variance of the original six TM bands.

b. Noise may be relegated to the less-correlated PC images.

c. Spectral differences between materials may be more apparent in PC images than in individual bands.

- **Disadvantage of the PCA Transformation:- [Aly 98]**

  a. This technique require a long time to find the result.

  b. The PCA is that it does not take discrimination of classes in to consideration.

  However the (PCA) can be used for the following application:-

  - Effective classification of land use with multi-band data.

  - Color representation or visual interpretation with multi-band data.

  - Change detection with multi-temporal data.

  - Compression of multi-band data.

  To study the PCA there are three steps required:

  1. Derivation of the variance-covariance matrix.

  2. Computation of the eigenvectors used for transformation can be derived from a covariance matrix (with non-standardized data) or a correlation matrix (with standardized data).

  3. Linear transformation of the data set.

2-2-1-3 Mathematical and theoretical basis of PCA [Lai 96]:-

PCA is a classical statistical method- this linear transform has been widely used in data analysis and compression. PCA is based on the statistical representation of a random variable. Suppose we have a random vector population x, where:

$$X = \begin{bmatrix} X_{1N} \\ X_{2N} \\ \cdot \\ \vdots \\ X_{NN} \end{bmatrix}$$ (2.1)

And the mean of that population is denoted by:

$$M_X = E\{X\}$$ (2.2)

Where E {.} is the expected value.

$$M_X \cong \frac{1}{M} \sum_{i=1}^{M} X_i$$ (2.3)

And the covariance matrix of the same data set is:

$$C_X = E\{(X - M_X)(X - M_X)^T\}$$ (2.4)

$$C_X = \frac{1}{M} \sum_{i=1}^{M} (X - M_X)(X - M_X)^T$$ (2.5)

Or equivalently:

$$C_X = \frac{1}{M} \left[\sum_{i=1}^{M} XX^T \right] - M_X M_X^T$$ (2.6)

Where T indicate transposition.

$$C_X = \begin{bmatrix} C_{1j} \\ C_{2j} \\ \cdot \\ \vdots \\ C_{ij} \end{bmatrix}$$ (2.7)

The components of C_x, denoted by C_{ij} represent the covariance between the random variable components X_i and X_j. The components C_{ij} is the variance of the components X_i.

The variance of a component indicates the spread of the component values a round its mean value. If two components X_i and X_j of the data are uncorrelated, their

covariance is Zero ($C_{ij} = C_{ji} = 0$). The covariance matrix is by definition, always symmetric.

From a symmetric matrix such as the covariance matrix, we can calculate an orthogonal basis by finding its eigenvalues and eigenvectors. The transformation matrix consist of eigenvectors of the covariance matrix is giving by:

$$A = \begin{bmatrix} e_{1n} \\ e_{2n} \\ . \\ : \\ e_{nn} \end{bmatrix} \qquad (2.8)$$

Where A is unity matrix (i.e. $A^{-1} = A^T$), e_{ij} is the jth component of the ith the eigenvector.

The Hotelling transform then consists simply of multiplying a centralized image vector, ($X-M_x$), by A to obtain a new image vector Y:

$$Y = A \left(X - M_X \right) \qquad (2.9)$$

Where M_x is the mean vector population and the rows of A are formed from the normalized eigenvector of the covariance matrix C_x.

The covariance matrix must be diagonalized as follows:

$$C_y = A C_x A^T = \begin{bmatrix} \lambda_1 & . & . & . & 0 \\ . & \lambda_2 & . & . & : \\ : & . & . & . & : \\ . & . & . & . & . \\ 0 & . & . & . & \lambda_{N^2} \end{bmatrix} \qquad (2.10)$$

From Equation (2.10) we can obtain that:

- The terms of the main diagonal are not zero.

- The elements of Y are uncorrelated.

- Each eigenvalue (λ_i) is equal to the variance of the ith element of Y along eigenvector e_i.

So each eigenvector (λ_i) corresponds to the Variance of a new PC image, and $\lambda_1 > \lambda_2 > .... > \lambda_{N^2}$, where λ_i represent the contrast of the image.

The eigenvalue are often called components (i.e. λ_1 may be referred to as PC1). The eigenvalue contain important information. The sum of the diagonal elements of the covariance matrix is called the trace represents the sum of all the characteristic roots of the covariance matrix. For orthogonal transformation, X can be reconstructed by:

$$X = A\,Y + M^T \tag{2.11}$$

Where Y is the amount of the characteristic vectors that must be added to the means of the vectors in order to produce estimation to the original image vector, called the scalar multipliers. The scalar multipliers are determined by:

$$Y = \sum_{i=1}^{N^2} W_i\,(X_i - M_X)^T \tag{2.12}$$

Where W_i represent the weighting coefficients, obtained by dividing the elements of the vector (V_i) by its largest value.

The correlation is the ratio of the covariance of two variable to product of their standard deviation this is known the degree of interrelation between two variables K and L.

$$r_{KL} = \frac{COV_{KL}}{\delta_K \delta_L} \tag{2.13}$$

where:

r_{KL} is Correlation between pixel value in band K and L

COV_{KL} the covariance between pixel value in band K and L

K is the band of imagery

L is the another band of imagery

δ is the standard deviation

The value of r_{KL} is ranged from +1 to -1

A correlation coefficient of +1 means perfect relationship between the brightness values in two of the band (as one band pixel increase in value the other band also increased). A correlation of -1 means that one band was inversely related to the other (As brightness value in one band increased in value corresponding pixels in the other band decrease in value). A correlation coefficient of zero suggests that there is no linear relationship between the two bands.

2-2-1-3 Description of PCA:

This transformation can be shown best by considering two-dimensional distribution of pixel values obtained by two TM bands   [Lai 96].If the bands are highly correlated, the ellipse will be very eccentric whereas, for less correlated bands, the ellipse is more symmetrical, the spread of the distribution of points is an indication of the correlation and quality of information associated with both bands [Gibson: 00].If the two variables X_1 and X_2 are perfectly correlated then measurements on X_1 and X_2 will plot as a straight line X_1 against X_2 then this transformation could be conveyed into one line AB as shown in figure (2-2).

If X_1 and X_2 are not perfectly correlated then we get a scatter plot; however, it is possible to create new axes, termed "PCs" by means of a translation, and a rotation direction. So that there is a dominant which can be chosen as the major axis AB and 2nd minor axis CD draw at right angles to the major axis. So, a graph of AB and CD instead of X_1 and X_2 – axes might, in some causes prove more revealing of structures that are present with in the data [Aly 98].

In fact the goal of PCA is to translate or rotate the original axes, so that the original brightness values on axes X_1 and X_2 are redistributed on to a new set of axes X'_1 and X'_2, Equation (2-14), there is relation between the original axes and the new set of axes:-

$$X'_1 = X_1 - \mu_1 \, , \, X'_2 = X_2 - \mu_2 \qquad (2\text{-}14)$$

Where: (μ_1, μ_2) is the mean of original scatter plot.

The origin of the new coordinate system X_1 and X_2 now lies at the location of both means (μ_1, μ_2) in the original scatter of point as shown in figure (2-3) [Laith: 96].
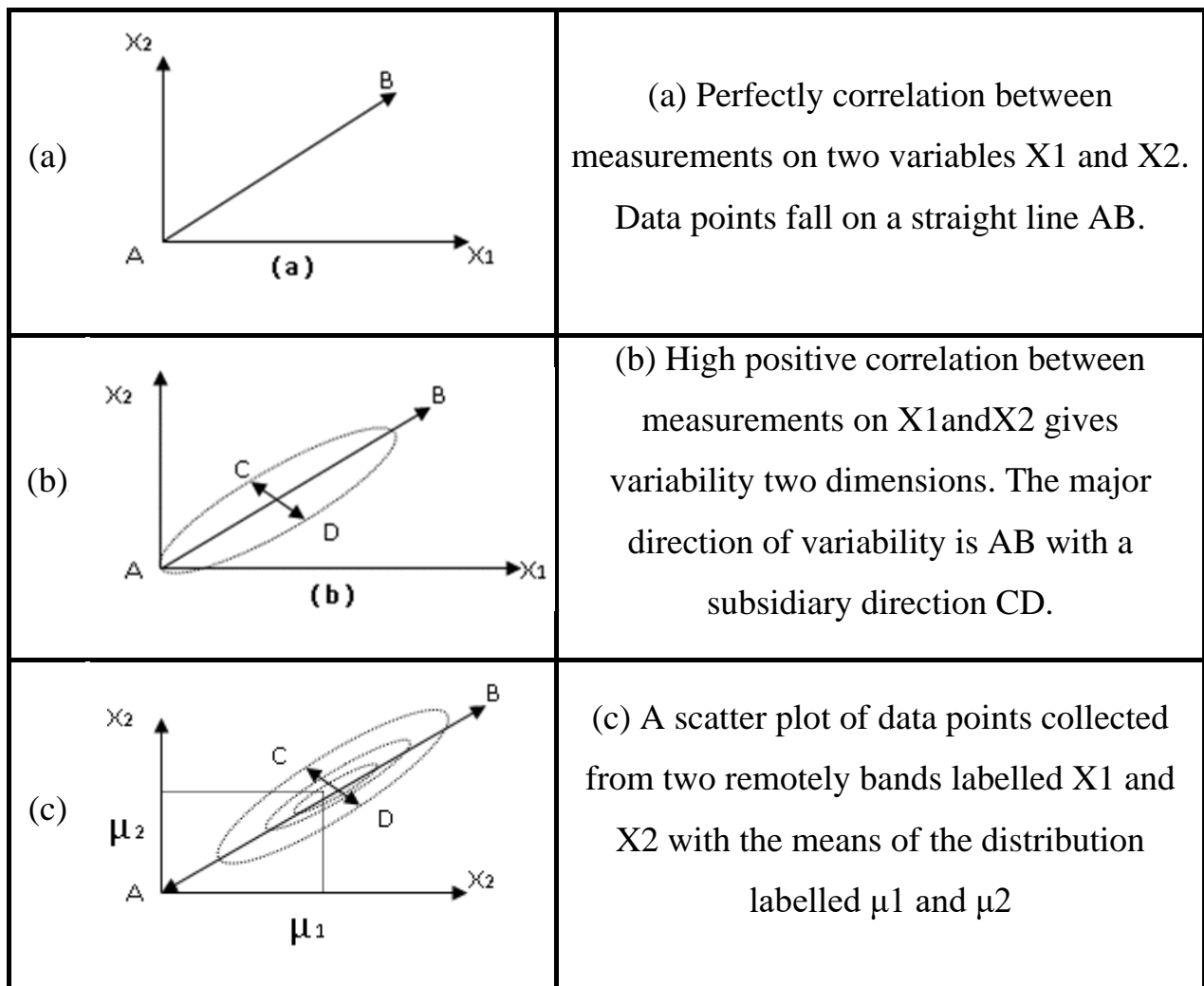

(a) [scatter plot showing line AB]	(a) Perfectly correlation between measurements on two variables X1 and X2. Data points fall on a straight line AB.
(b) [scatter plot showing ellipse with AB and CD]	(b) High positive correlation between measurements on X1andX2 gives variability two dimensions. The major direction of variability is AB with a subsidiary direction CD.
(c) [scatter plot showing ellipse with means]	(c) A scatter plot of data points collected from two remotely bands labelled X1 and X2 with the means of the distribution labelled μ1 and μ2

Figure (2-2) Describe the correlation between two dimension distributed of pixel values obtained by two correlated bands. [Aly: 98]

The PCA expresses the input digital numbers in the original bands in terms of the new PC axes. Although the visualization of the PCs is simple, in order to create the PC axes, it is necessary to calculate the length of the PC axes and their direction [Gib 00]. These are computed by determining the eigenvalues (length) and eigenvectors (direction) from the variance – covariance matrix.

The X-coordinates system might then be rotated some degrees about its new origin (μ_1 ,μ_2) in the new coordinate system so that the first axes X_1 is associated with

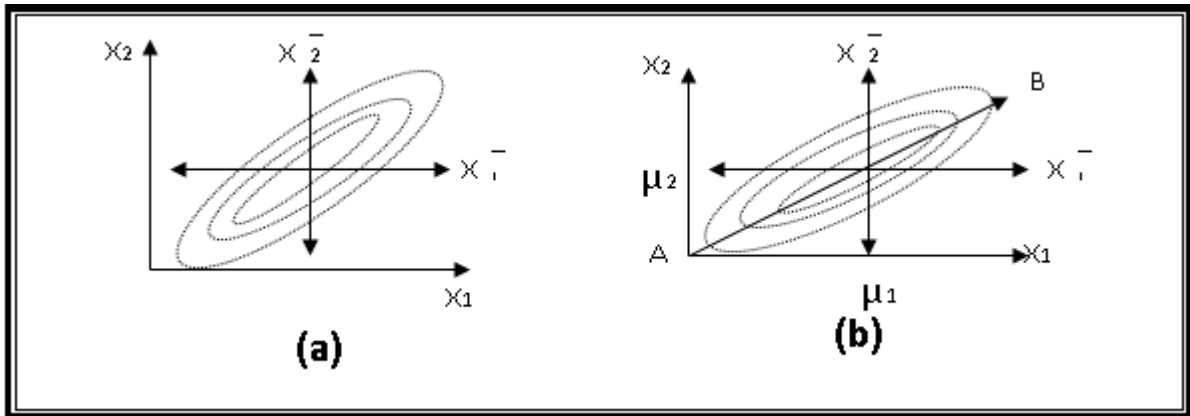the maximum amount of the variance in the scatter of points as shown in figure (2-4).

Figure (2-3): Distribution of the brightness values associated with each pixel in each band with the location of the means μ_1 and μ_2 in a new coordinate system is created by shifting the axes to an $\overline{X}$ system [Lai 96].
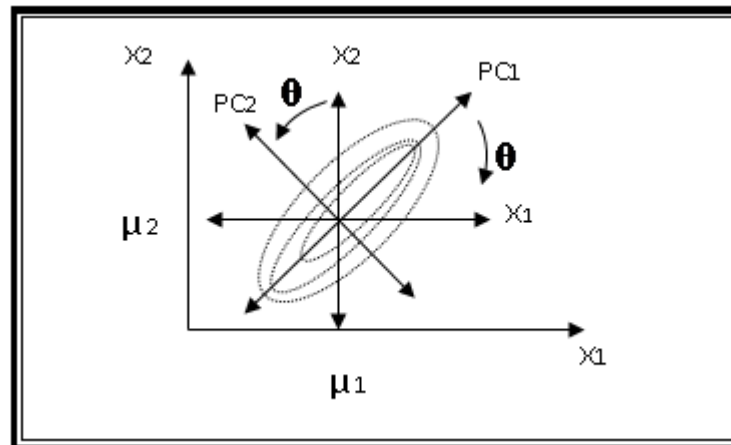

Figure (2.4): The new coordinate system rotated some Θ degree about the new origin in the new coordinate system [Lai 96].

Thus, the major and minor axes of the ellipsoid of point in that the band X_1 and X_2 are called the (PCs). So, the first principal component (PC$_1$= λ_1) and the second principal component (PC$_2$= λ_2) which is perpendicular where λ_1, λ_2…and λ_n known as the Eigen-values of variance-covariance matrix. The same procedure can be used to produce images for the remaining PCs [Jen 86].

2-3   Image Enhancement:

Image Enhancement is one of the most important techniques in image research. It is simple and most appealing area among all the digital image processing techniques, It is important to keep in mind that enhancement is a very subjective area of image processing Improvement in quality of these degraded images can be achieved by using application of enhancement techniques [Raj 11, Juw 08].

The aim of image enhancement is to improve the interpretability or perception of information in images for human viewers, or to provide 'better' input for other automated image processing techniques, it helps analyses background information that is essential to understand object behavior without requiring expensive human visual inspection. Carrying out image enhancement understanding under low quality image is a challenging problem because of these reasons [Man 13].

Image Enhancement (IE) is an indispensable tool for researchers in a wide variety of fields including (but not limited to) medical imaging, art studies, forensics and atmospheric sciences. Image enhancement techniques may be suitable for one problem and may be inadequate for another. For example forensic images/videos employ techniques that resolve the problem of low resolution and motion blur while medical imaging benefits more from increased contrast and sharpness [Raj11].

Various enhancement schemes are used for enhancing an image which includes gray scale manipulation, filtering and Histogram Equalization (HE). Histogram equalization is one of the well-known image enhancement technique. It became a popular technique for contrast enhancement because this method is simple and effective [Raj 11]. Histogram equalization technique have been adopted in this research as an enhancement technique for the purpose of determining the training area as the first step in image supervised classification.

Visual analysis and interpretation is an efficient method for extracting information for remotely sensed images in the form of standard photo-graphic prints. If the images is digital in nature, such as satellite acquired images considered in this

study, computer programs can be used to manipulate and display the image data and to generate picture which satisfy the particular needs of the interpreter. [Juw 08]

Digital image enhancement techniques have become a major process in presenting spectral characteristic of earth materials. Minerals, rocks, soil, land-cover, and other earth materials can be discriminated and identified according to their relative reflectance in the spectral domain. Statistical and mathematical manipulation make remote sensing images in their digital format more useful in geologic, geomorphic, land- use, and ground water studies as well as in other applications. [Kim 97]

The term enhancement is used to indicate the alteration of the appearance of an image in such a way that the information contained in that image well be more readily interpreted by the viewer in term of his particular needs. No single standard method of enhancement can be said the "best", because the results are ultimately evaluated by human beings who make subjective judgments as to whether a given image enhancement is useful and different method may be used for different purposes. Principal component, color composite, rationing, and hue saturation intensity are the most usable techniques, frequently accompanied by filtering and stretch enhancement, also, the nature of each image in terms of the distribution of pixel values over 0-255 range will change from one area to another, thus enhancement technique suited to one image (for example, covering an area of forest) will differ from the techniques applicable to another kind of area. [wan 99]

2-3-1 Color Fundamentals:

The colors that humans and most animals perceive in an object are determined by the nature of the light reflected from the object For example, green objects reflect light with wave lengths primarily in the range of $500 - 570$ nm while absorbing most of the energy at other wavelengths. Chromatic light spans the electromagnetic spectrum from approximately 400 to 700 nm. A human color vision is achieved through 6 to 7 million cones in each eye

The purpose of a color model is:

- To facilitate the specification of colors in some standard.

- In essence, a color model is a specification of a coordinate system and a subspace within that system where each color is represented by a single point.

- Most color models are oriented either toward specific hardware or toward applications.

2-3-1-1 The RGB Model: [Gon 87]

In color image processing the color of a pixel is usually given as three values corresponding to the tri-stimulus values R (red), G (green) and B (blue). Experiments has shown that the number of blue sensitive cones is much less than the number of red or green sensitive cones. Figure (2-5) show the areas of the visible spectrum in which the three kinds of cones respond.

A model of color space can be derived from the idea that colors are formed by adding together differing amount of red, green, and blue light. Figure (2-6) shows geometrical representation of the RGB cube, the origin is at the vertex of the cube marked "black" while the axes are black-red, black-green, and black-blue.
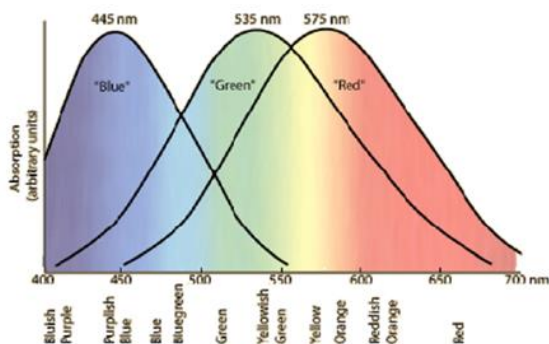
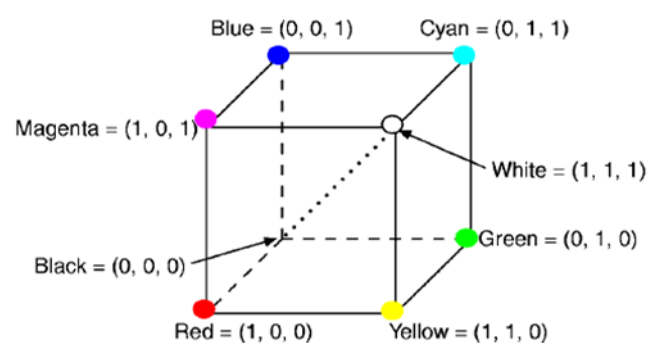**Figure (2-5) The areas of the visible spectrum in which the three kinds of cones respond.**

Figure (2-6) The geometrical representation of the RGB representation of the RGB cube

There are other opinions on coloring, but the tri-stimulus theory is an attractive one, not merely because it is simple but it provides the idea that color can be formed by just adding red, green, and blue light in various combination.

A color is specified by giving its coordinates along these three axes, these coordinates are termed (R ,G ,B) triples, notice that white light can be formed by the addition of maximum red, maximum green, and maximum blue light. The line joining the black and white vertices of the cube represents color formed by the addition of equal amount of red green and blue light, these are shades of gray.

The color television screen is composed of an array of dots, each of which contains red, green, and blue sensitive phosphors. Colors on the screen are formed by exciting the red, green and blue phosphor in differing proportions. If the portions of the added red, green, and blue were equal at each point a black and white or monochrome picture would result. A color picture is obtained when the amount of red, green, and blue at each point are unequal. The RGB model is of interest primarily because normally used in the study and interpretation of remotely sensed images, in color TV monitors, and in many raster displays.

2-3-1-2 Additive Primary Colors:

Additive color mixing: adding red to green yields yellow; adding red to blue yields magenta; adding green to blue yields cyan; adding all three primary colors together yields white.

To form a color with RGB, three light beams (one red, one green, and one blue) must be superimposed (for example by emission from a black screen, or by reflection from a white screen). Each of the three beams is called a component of that color, and each of them can have an arbitrary intensity, from fully off to fully on, in the mixture.

The RGB color model is additive in the sense that the three light beams are added together, and their light spectra add, wavelength for wavelength, to make the final color's spectrum. Zero intensity for each component gives the darkest color (no light, considered the black), and full intensity of each gives a white; the quality of this white depends on the nature of the primary light sources, but if they are properly balanced, the result is a neutral white matching the system's white point.

When the intensities for all the components are the same, the result is a shade of gray, darker or lighter depending on the intensity. When the intensities are

different, the result is a colorized hue, more or less saturated depending on the difference of the strongest and weakest of the intensities of the primary colors employed.

When one of the components has the strongest intensity, the color is a hue near this primary color (reddish, greenish, or bluish), and when two components have the same strongest intensity, then the color is a HUE of a secondary color (a shade of cyan, magenta or yellow). A secondary color is formed by the sum of two primary colors of equal intensity: cyan is green + blue, magenta is red + blue and yellow is red + green. Figure (2-7) represent the RGB cube.
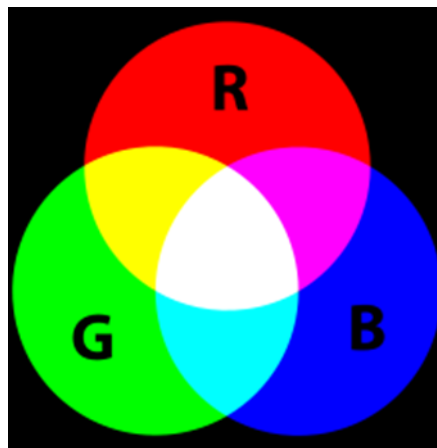
Figure (2-7) the geometrical representation of the RGB cube.

Every secondary color is the complement of one primary color; when a primary and its complementary secondary color are added together, the result is white: cyan complements red, magenta complements green and yellow complements blue.

The RGB color model itself does not define what is meant by red, green, and blue colorimetric-ally, and so the results of mixing them are not specified as absolute, but relative to the primary colors.

2-3-2 Image Histogram:

Histogram is one of the important features which are very related to image enhancement. The histogram does not only gives us a general overview on some useful image statistics (e.g. mode, and dynamic range of an image), but it also can be used to predict the appearance and intensity characteristic of an image. If the

histogram is concentrated on the low side of the intensity scale, the image is mostly a dark image. On the other hand, if the histogram is concentrated on the high side of the scale, the image is mostly a bright image. If the histogram has a narrow dynamic range, the image usually is an image with a poor contrast [Gonzalez 02].

Image Histograms are mostly used to describe the statistical distribution of the gray levels in an image. The graphic display of a set of data that shows the frequency of occurrence the (vertical axis) of individual measurements or values (along the horizontal axis) [Jensen: 86].

Image Histogram is referred to as the probability density function (PDF) of the image. Therefore, the probability that an image level repeats itself "H (n)" time is given by:

$$P(n) = \frac{H(n)}{MN} \qquad\qquad (2\text{-}15)$$

Where MN is the total number of pixels in a two-dimensional image array. [Laith: 96]

The histogram is a useful graphic representation of the information contents a remotely sensed image. Histograms provide the reader with an appreciation of the quality of the original data (e.g., whether it is low in contrast, high in contrast, or multi-modal in nature) .

Image contrast enhancement [Kim: 97, Wang: 99] is a classical problem in image processing and computer vision. Image enhancement is considered as a preprocessing step in many areas like video/image processing applications [Pei: 04, Pizer: 03] speech recognition, texture synthesis etc. Enhancement techniques mainly fall into two broad categories: spatial domain methods and frequency domain methods [Gonzalez: 02]. Spatial domain techniques are more popular than the frequency based methods, because they are based on direct manipulation of pixels in an image. Myriad spatial domain methods have been developed for visualizing the effect. Some of these methods uses simple linear or non-linear intensity level

transformation functions, whereas others use complex analysis of different image features such as the edge and connected component information.

Contrast enhancement problem in digital images can be resolved using various methodologies, but Histogram Equalization (HE) [Gonzalez: 02] technique is the widely used one.

2-3-3 Histogram Equalization:

It is an automatic enhancement technique which produce an output (enhanced) image that has a near uniformly distributed histogram. [Juw 08]

For continuous functions, the intensity (gray level) in an image may be viewed as a random variable with its probability density function (PDF). The PDF at a gray level r represents the expected proportion (likelihood) of occurrence of gray level r in the image. A transformation function has the form:

$$s = T(r) = (L - 1) \int_0^r p_r(w)dw \qquad (2\text{-}16)$$

Where w is a variable of integration. The right side of this equation is called cumulative distribution function (CDF) of random variable r. For discrete gray level values, we deal with probabilities (histogram values) and summations instead of probability density functions and integrals. Thus, the transform will be:

$$s = T(r_k) = (L - 1) \sum_{j=0}^{k} p_r(r_j) = (L - 1) \sum_{j=0}^{k} \frac{n_j}{M \times n} \qquad (2\text{-}17)$$

$$= \frac{(L-1)}{M \times N} \sum_{j=0}^{k} n_j \qquad k = 0,1,2, \ldots \ldots \ldots \ldots, L - 1 \qquad (2\text{-}18)$$

The right side of this equation is known as the cumulative histogram for the input image. This transformation is called histogram equalization or histogram linearization.

2-3-4 Selection of band combination of TM Data [Mic 86].

One obvious problem that may arise in making color composite images is the choice of the bands. The choice is non-trivial, since bands which can be selected from

the six TM bands may follow different ways. Moreover, selected band can be assigned different color

One well known and widely used approach to the problem of the choice is the through the use of the principle components of the images. For although, the first three principal components contain , in a statistical sense, as much information as can be presented using three colors, the best three bands are those that have the largest some of squared principal axes and hence that account for the largest total variance. The sum of squared principal axes is in fact equal to the trace of the covariance matrix.

The band triplet that accounts for the greatest variance found from the original variance- covariance matrix, simply, by selecting the three bands with the largest diagonal elements.

2-4   Image Classification:

Image classification refers to the computer-assisted interpretation of remotely sensed images. Although some procedures are able to incorporate information about such image characteristics as texture and context, the majority of image classification is based solely on the detection of the spectral signatures (i.e., spectral response patterns) of land cover classes. The success with which this can be done will depend on two things: [Har 15]

a- The presence of distinctive signatures for the land cover classes of interest in the band set being used.

b- The ability to reliably distinguish these signatures from other spectral response patterns that may be present.

There are two general approaches to image classification: supervised and unsupervised. They difference is in how the classification is performed.

In the case of supervised classification, the software system delineates specific land cover types based on statistical characterization data drawn from known examples in the image (known as training sites).

With unsupervised classification, however, clustering software is used to uncover the commonly occurring land cover types, with the analyst providing interpretations of those cover types at a later stage.

2-4-1 Supervised Classification: [Lai 96]

The first step in supervised classification is to identify examples of the information classes (i.e., land cover types) of interest in the image. These are called training sites.

The software system is then used to develop a statistical characterization of the reflectance for each information class. This stage is often called signature analysis and may involve developing a characterization as simple as the mean or the range of reflectance's on each band, or as complex as detailed analyses of the mean, variances and co-variances over all bands.

Once a statistical characterization has been achieved for each information class, the image is then classified by examining the reflectance for each pixel and making a decision about which of the signatures it resembles most. There are several techniques for making these decisions, called classifiers. Most Image Processing software will offer several, based on varying decision rules.

Various supervised classification methods may be used to assign an unknown pixel to one of these classes. Supervised classification involves a considerable amount of input from the image analyst and knowledge of the types of surface that are found in the stud-y area. This information can be obtained from the sensor.

2-4-1-1 Advantages and Disadvantages of supervised classification: [Lai 96]

- The advantages of supervised classification can be marked as follows:

  a- The analyst has control of a set, selected menu of informational categories tailored to a specific purpose and geographic region.

  b- Supervised classification is tied to specific areas of known identity, as provided through the process of selecting training areas.

    c- The operator may be able to detect serious errors by examining training data to determine whether they have been correctly classified.

- The disadvantages of supervised classification are:

    a. The analyst, in effect imposes a classification structure up on the data (recall that unsupervised classification searches for "natural" classes).

    b. Training data are often defined primarily on informational categories and only secondarily on spectral properties.

    c. Training data selected by the analyst may not be representative of conditions encountered throughout the image.

    d. Supervised classification may not be able to recognize and represent special or unique categories not represented in the training data.

2-4-1-2 The maximum likelihood classification algorithm: [Lai 96]

Maximum likelihood classification is the most common supervised classification method used with remote sensing image data. Bayes decision theory is a fundamental statistical approach to the problem of pattern classification. This based on the assumption that training area data sets have a normal distribution (Gaussian in nature), which involves the construction of probability contours.

Maximum likelihood rule a statistical decision criterion to assisting the classification of overlapping signatures; pixels are assigned to the class in which they have the highest probability of being a member. The general multivariate normal density is written as:

$$P(x) = \frac{1}{(2\pi)^{1/2}|\Sigma|^{1/2}} e^{(-\frac{1}{2}Y^T\Sigma^{-1}Y)} \tag{2-19}$$

Where

$$Y = X - \mu$$

P (x) define the probability of pixel vector of (d) elements (a pattern defined in term of features).

μ: is the d-component mean vector.

Σ: is the d by d covariance matrix.

T: is a superscript indicating transposition.

Σ^{-1}: is the inverse of the covariance matrix.

$|\Sigma|$: **i**s the determinant of the covariance matrix.

Generally, samples drawn from a normal distribution tend to fall in a single cloud or cluster, the mean vector determines the center of the cluster, and the shape of the cluster is determined by the covariance matrix and $(x-\mu)^T\Sigma^{-1}(x-\mu)$ is the contrast.

The principle axes represent the eigenvectors of Σ, and the eigenvalues determining the lengths of these axes.

The quantity:

$$r^2 = (x - \mu)^T\Sigma^{-1}(x - \mu) \qquad (2\text{-}20)$$

Called the squared Mahalanobis distance from x to μ.

The advantage of the Mahalanobis classifier over the maximum likelihood procedure is that it is faster and yet retains degree of direction sensitivity via the covariance matrix Σ.

The volume of hyperellipsoids measures the scatter of the samples about the mean, it is given by:

$$V = V_d \, |\Sigma|^{1/2} r^d \qquad (2\text{-}21)$$

Where V_d is the volume of a d-dimensional unit hypersher:

$$V_d = \begin{cases} \dfrac{\pi^{d/2}}{\left(\frac{d}{2}\right)!} \dots\dots\dots\dots\dots \; if \; d \; is \; even \\[4mm] \dfrac{2^d \pi^{\frac{d-1}{2}}\left(\frac{d-1}{2}\right)!}{d!} \dots\dots\dots\dots\dots if \, d \; is \; odd \end{cases} \qquad (2\text{-}22)$$

For given dimensionality, the scatter of the samples varies directly with $|\Sigma|^{1/2}$, the cost of carrying out these computation can be saved by avoiding evaluating the

exponential term in equation (2-19). Taking the logarithm of both sides of equation (2-19) does this.

$$\ln(P(x)) = -0.5 d\ln(2\pi) - 0.5\ln|\Sigma| - 0.5(x-\mu)^T\Sigma^{-1}(x-\mu) \qquad (2\text{-}23)$$

The rank order unaffected if this expression is multiplied by 2 and the constant term ((0.5dln (2Π)) is dropped and the equation (2-23) can be written as :

$$-2\ln(P(x)) = \ln|\Sigma| + (x-\mu)^T\Sigma^{-1}(x-\mu) \qquad (2\text{-}24)$$

The effectiveness of maximum likelihood classification depends upon reasonably accurate estimation of the mean vector m and the covariance matrix Σ for each spectral class.

The maximum likelihood classifier is generally considered to be the most powerful but is also considered the most computer intensive. According to this algorithm, Pixel 1 belongs to class A, Pixel 2 to class B and Pixel 4 to class C. Pixel 3 has a higher probability of belonging to class B than class C, (Note that dispersion for the pixel in class B is greater than in class C; An unknown pixel equidistant from both therefore has a greater affinity with class (B)). Shows in figure (2-8).
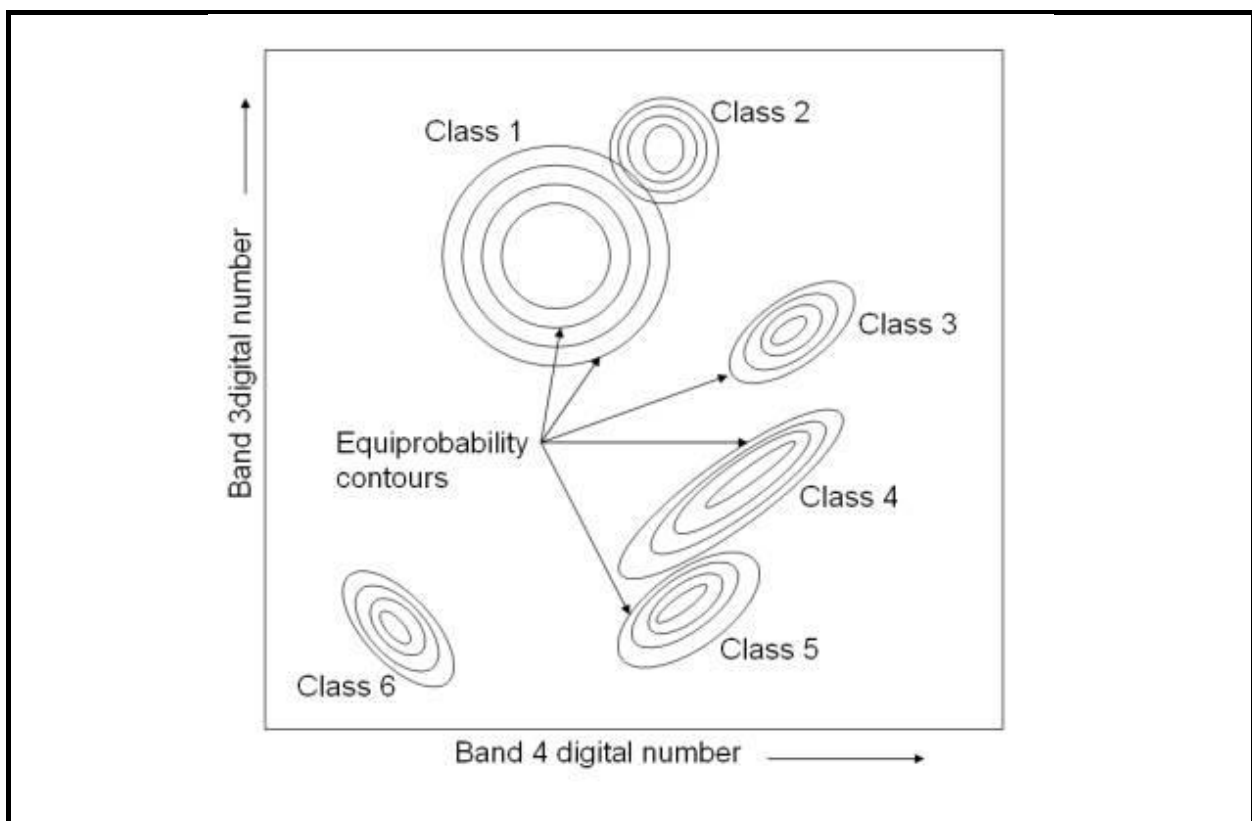
Figure (2-8) classification procedure of maximum likelihood

2-4-1-3 Training Area: [Lai 96]

One of the most important concept of pattern recognition in remote sensing is the definition of the classes into which the data to be categorized. The accuracy of a supervised classification analysis will depend up on two factors: -

1- The representativeness of the estimates of the number and statistical nature of the spectral classes present in the image data.

2- The degree of departure from the assumptions on which the classification technique is based.

Also, the important factors, which indicate the validity of statistical estimates, depends on two factors:

a. Size of the sample, which is related to the number of the spectral bands.

b. Representativeness of the sample.

It is important to note:

I.   The definition of a certain class is always follow other classes used in the same classification.

II.   The type of classes involved in out lookup table must be separable from others.

III. Have informational values.

IV.   The spectral response of the chosen class should be sufficiently distinct from the response of other classes to avoid the overlapping of these classes.

2-4-2 Unsupervised Classification: [Lai 96]

In contrast to supervised classification, where we tell the system about the character (i.e., signature) of the information classes we are looking for, unsupervised classification requires no advance information about the classes of interest. Rather, it examines the data and breaks it into the most prevalent natural spectral groupings, or clusters, present in the data. As opposite to the supervised the unsupervised classification requires only a minimal amount of initial input from the analyst. The

analyst then identifies these clusters as land cover classes through a combination of familiarity with the region and ground truth visits.

2-4-2-1 Advantages and disadvantages of unsupervised classification:

- Advantages of the unsupervised classification is:

    a. No extensive prior knowledge of the scene is required.

    b. The opportunity for human error is minimized.

    c. Unique classes are recognized as distinct units.

- Disadvantages of the unsupervised classification are:

    a. Unsupervised classification identifies spectrally homogeneous classes within the data, these classes do not necessarily correspond to the informational categories that are of interest to the analyst.

    b. The analyst has limited control over the menu of classes and their specific identities.

    c. Spectral properties of specific informational classes will change over time (on a seasonal basis, as well as over the years).

CHAPTER THREE

Experimental Results

3-1 Introduction:

This chapter is devoted to present the yielded results depending on the theoretical basis as described in chapter two to reach to the aim of this work (classification of multispectral images). As we described before, the classification of remotely sensed image regions involves the assignment of each image point a label which refers to a certain pattern in the real world scene. These set of values which are associated with each image point are usually referred to as a pattern (class). The classification process can be described as a form of pattern recognition.

Pattern recognition is carried out by a series of statistical measurements extracted from each pattern on multispectral on multispectral data by means of qualitative and quantitative approaches. Maximum Likelihood is a supervised classification method which is based on the Bayes theorem. It makes use of a discriminant function to assign pixel to the class with the highest likelihood. Class mean vector and covariance matrix are the key inputs to the function and can be estimated from the training pixels of a particular class. In this study, we used Maximum Likelihood to classify land use/covers recorded from Landsat 8.

3-2 The Study Area

The remotely sensed imagery was presented by the Iraqi Geological Survey organization. The imagery was captured by the Landsat 8 (Worldwide Reference System (WRS-2) path 169 row 37), the provided scene is for Baghdad state on the 25th of September 2015. The scene consists of six bands in 1003×989 pixels with an 8 bit gray level, the wavelength of each band has been clarified in the table (3-1), and the data corrected and projected to UTM zone 38 Z.

This area was well suited for the study as it contains various geographical land use and land cover, it contains Deep Water, Population, Trees, River, Streets, and various lands (Harvested lands, Barren Lands, Herbals Lands)
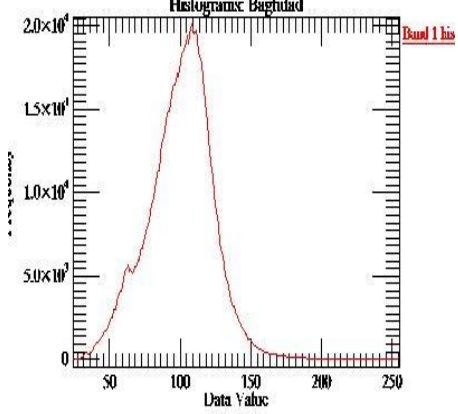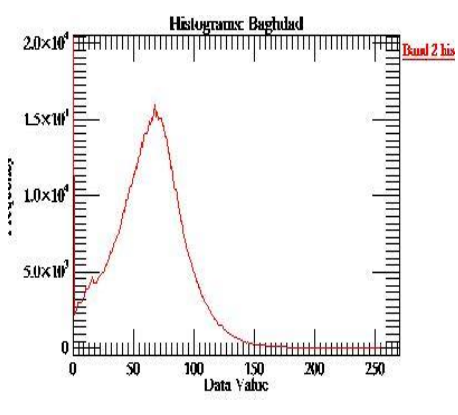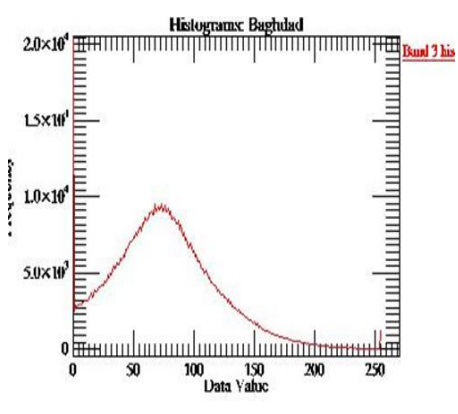
In this chapter, we attempt to apply the classification methods on the imagery data to reach a classified image that can clarify the component of the Baghdad scene.

Table (3-1) Bands spectral and spatial resolution

Bands	Wavelength (µm)	Resolution (m)
Band 1	0.450 - 0.515	
Band 2	0.525 - 0.600	
Band 3	0.630 - 0.680	30×30
Band 4	0.845 - 0.885	
Band 5	1.560 - 1.660	
Band 7	2.100 - 2.300	

Figure (3-1) shows each band as a gray level image, and the histogram distribution plot for each band. The histogram distribution reflects the contrast in the image, it is clear from figure (3-1) that the contrast in a visible bands more clarity than in the IR bands, most value of the pixel distribution in the IR band aggregates toward the white region (pixel value = 255) so that the IR bands seem to be lighter and it is difficult to discriminate between the classes in these bands.

Among the too many existed statistical parameters, the mean, standard deviation and variance -co-variance have the superiority in measuring the central tendency. These parameters, sometimes, are even more useful, from a remote sensing standpoint, than the co-variation and correlation measures among the several available bands. They can provide insight into image redundancy and quality.

Band 1		
Band 2		
Band 3		

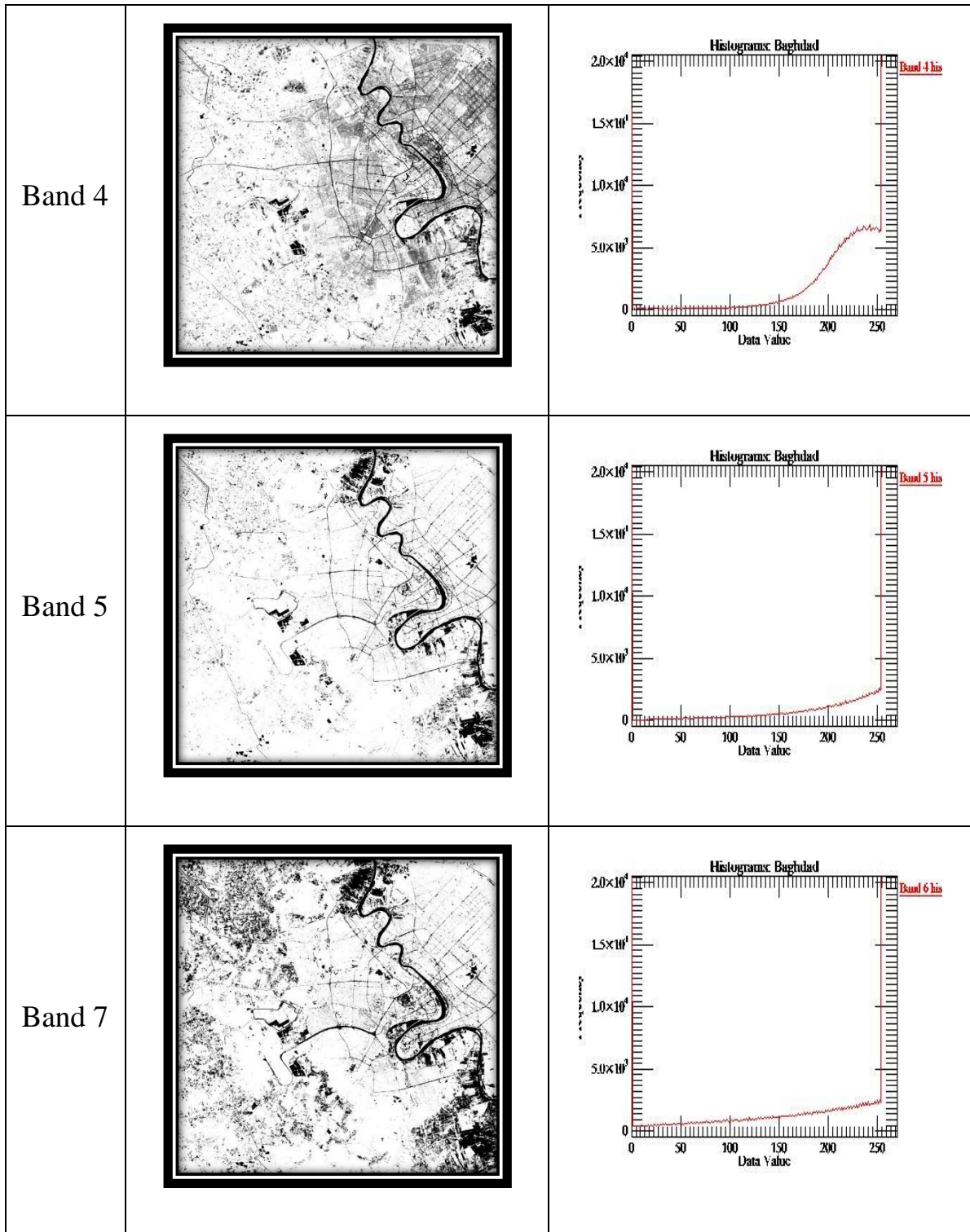|		
Band 4		
Band 5		
Band 7		

Figure (3-1) TM bands and histogram distribution plot of bands for Baghdad state with Landsat 8

The simple univariate statistics for our data are tabulated in table (3-2). This table show that band1 exhibits the smallest variance (536.5) and the smallest range of brightness value (231), from (24 -255). Conversely band7 has the largest variance (5775.2) and widest range of brightness (255). The variance with mean value may be reflect on the quality of the image. The variance and means look like the torque in

physics. So that we can see that the image with low variance and mean value near the middle range value (like band1) has more quality than the image with high variance and mean value near the edge of the minimum or maximum value (like IR bands).

Unfortunately, these univariate statistics don't provide any useful information concerning whether or not the spectral measurements in the six bands vary together or are completely independent.

Table (3-3) give the correlation matrix for the six bands of TM images for Baghdad scene. This table shows that the correlation between visible bands is highly correlated, the highest one between band 1 and band 2 (0.97), this means that there are amount of redundancy in the information contents among these visible bands. The IR bands, exhibits a low correlation between all bands for Baghdad scene, but the lowest one between band 4 and band 1 (0.36).

Table (3-2) Univariate statistics for Baghdad scene composed of six bands.

Band	Basic Statistics				
	Min	Max	Mean	Standard Div.	Range
1	24	255	100.15	23.16	231
2	0	255	62.38	30.21	255
3	0	255	68.14	46.66	255
4	0	255	232.30	43.93	255
5	0	255	238.73	48.84	255
7	0	255	214.07	75.99	255

Band	The variance-covariance matrix for Baghdad scene					
	1	**2**	**3**	**4**	**5**	**7**
1	536.5					
2	678.5	912.5				
3	986.1	1368.8	2176.9			
4	369.1	546.7	830.1	1929.7		
5	622.8	794.1	1051.5	1607.4	2385.7	
7	1344.9	1736.8	2474.8	1529.8	2950.5	5775.2

Table (3-3) the correlation matrix for the TM bands.

Correlation	Band 1	Band 2	Band 3	Band 4	Band 5	Band 7
Band 1	1.00					
Band 2	0.9698	1.00				
Band 3	0.9125	0.9712	1.00			
Band 4	0.3628	0.4120	0.4050	1.00		
Band 5	0.5505	0.5382	0.4614	0.7491	1.00	
Band 7	0.7641	0.7566	0.6979	0.4582	0.7948	1.00

To achieve the process of classification using maximum likelihood method, it is important to choose adequately the training area for the classes in our Baghdad scene bands. It is clear from these bands that the quality of these bands seems to be poor and this effect on the selecting the training area correctly. Now the coloring method must be applied to help the user to optimize the selection of the region of interest (ROI).

The RGB coloring method is adopted for this purpose as an unsupervised classification to make the differentiation between different classes more clarity.

3-3 RGB Coloring:

The first step in the RGB color transforms require three bands for input. The RGB color transform uses this input to convert three-band red, green, blue (RGB) images to one of several specific color spaces. Figure (3-2) shows an example of color image for Baghdad scene for a different RGB component of the original band for Baghdad scene. As we see, there are many choices for selecting the three bands between the six bands, but the traditional method of choosing the three bands comes from choosing the three bands which have the largest variance value.

In Baghdad scene the three bands which have the largest variance value are bands (3, 5, 7). Figure (3-3) shows two color images for Baghdad scene using the RGB model from the bands which have the first two largest variance value (bands 7,

5, 3, sum of variance = 10337.8) and (bands 7, 5, 4, sum of variance = 10090.6) respectively.
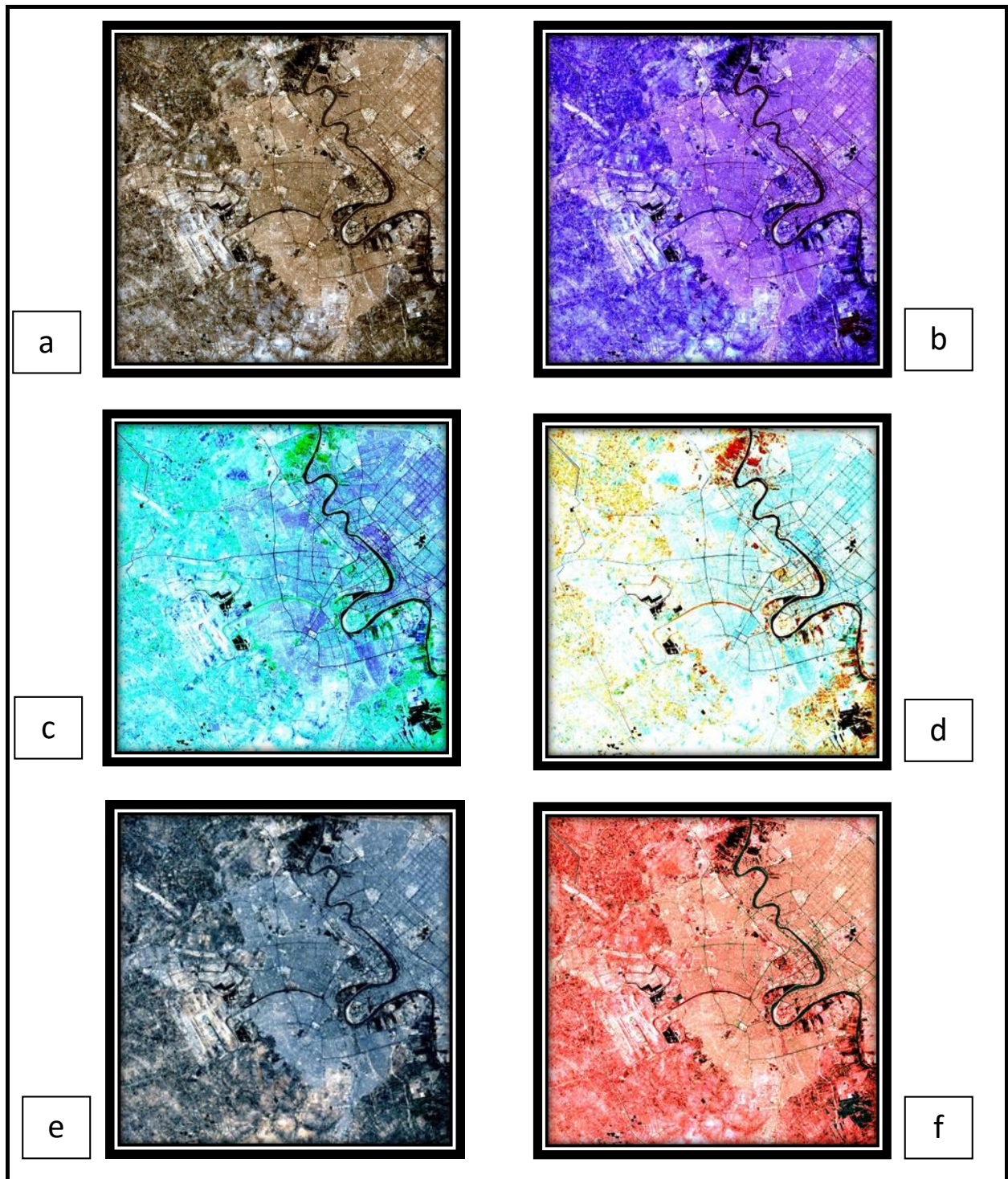

Figure (3-2) Color for Baghdad scene using the RGB model from triplet selecting bands (a-bands 123, b- bands 124, c- bands 345, d- bands 457, e-bands 321, f- bands 531)
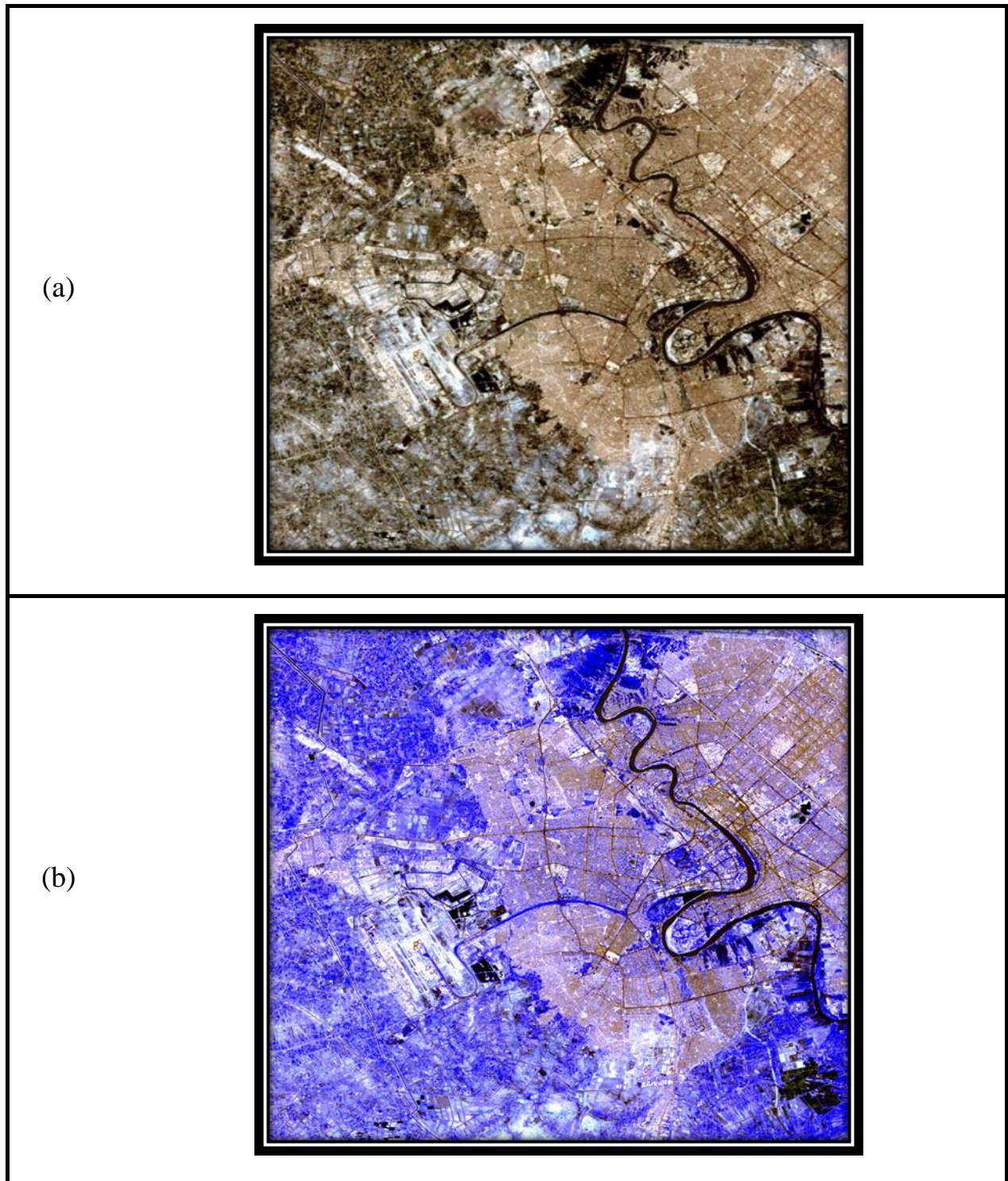
Figure (3-3) shows two color images from Baghdad using the RGB model from the bands which have the first two largest variance value.

Although the color image constructed from the bands which have the largest variance value (bands 3, 5, 7, sum of variance = 10337.8), but the problem still exist and need to resolve because these bands have redundancy due to the correlation

between these bands. To overcome this problem, the widely used approach to this problem is through the use of principal component images.

3-4 Principle Component Analysis:

As mentioned before that one of the most advantages of applying principle component analysis come from that of most of the variance in multispectral data set is compressed into one or two PC images, since the first few images contain essentially all information present in the original spectral bands. Moreover, the principle component images are spectrally uncorrelated. Table (3-4) show the eigenvalue and relative eigenvalue of the covariance matrix.

Table (3-4) Eigenvalue and relative eigenvalue of the covariance matrix

Principle component	Eigenvalue	Relative Eigenvalue	accumulative variance %
PC1	10279.90	0.7495	74.95%
PC2	1908.46	0.1391	88.86%
PC3	1234.66	0.0900	97.86%
PC4	223.37	0.0163	99.49%
PC5	61.72	0.0045	99.94 %
PC6	8.42	0.0006	100%

Table (3-4) shows that the first component hold about (74.955%) of the variability in the data of the scene, where the second component hold about (13.913%) of the variability in the data, and the third component hold (9.001%). This indicates that about (97.8601%) of the variability in the data are lies in the first three components. The last three components (4-6) hold only about (2.14%) of the variability. Table (3-5) shows the values of eigenvectors have been used for constructing the principal component images for the Baghdad TM scene.

Table (3-5) the eigenvector matrix for the TM bands.

Eigenvectors	E1	0.7202	0.4142	0.2732	0.3675	0.2521	0.1910
	E2	-0.1371	0.5048	0.6240	-0.4658	-0.2765	-0.2090
	E3	0.5483	-0.1195	0.5480	0.5362	0.2736	0.1501
	E4	0.4014	-0.7195	0.4604	-0.0473	-0.1962	-0.2616
	E5	-0.0288	0.2039	-0.1539	0.5451	-0.3304	-0.7264
	E6	0.0003	0.0075	0.0084	0.2471	-0.7985	0.5489

The result of this table shows that the first principle component image which is defined by the first eigenvector summarizes the information that is common to all bands for Baghdad scene.

Table (3-6) presents the correlation between each band and each component. The results of this table show that all factor loading for the first principle component have high correlation, it is also clear that the correlation between each band in Baghdad scene decreases gradually with the remaining components.

Table (3-7) presents the correlation between each component with all constructed components, the results shows that this correlation is weak compared between the results obtained in table (3-3).

The principle component images for Baghdad scene can be seen in figure (3-4), as its clear visually from these PC images that the first component has the highest clarity among the other components.

Table (3-6) shows the correlation between each PC and Each band.

Correlation	PC1	PC2	PC3	PC4	PC5	PC6
Band 1	0.8469	-0.4707	-0.2184	0.1396	0.2286	-0.0833
Band 2	0.8601	-0.4729	-0.309	0.0682	0.0669	0.0628
Band 3	0.8148	-0.5063	-0.3982	-0.0089	-0.1075	-0.0253
Band 4	0.5922	0.5541	-0.4405	-0.1726	0.0254	0.0095
Band 5	0.8335	0.3777	0.0874	0.1757	-0.0351	0.0104
Band 7	0.9662	-0.1505	0.2568	-0.1257	0.0013	0.0055

Table (3-7) shows the correlation between each PC and the other components

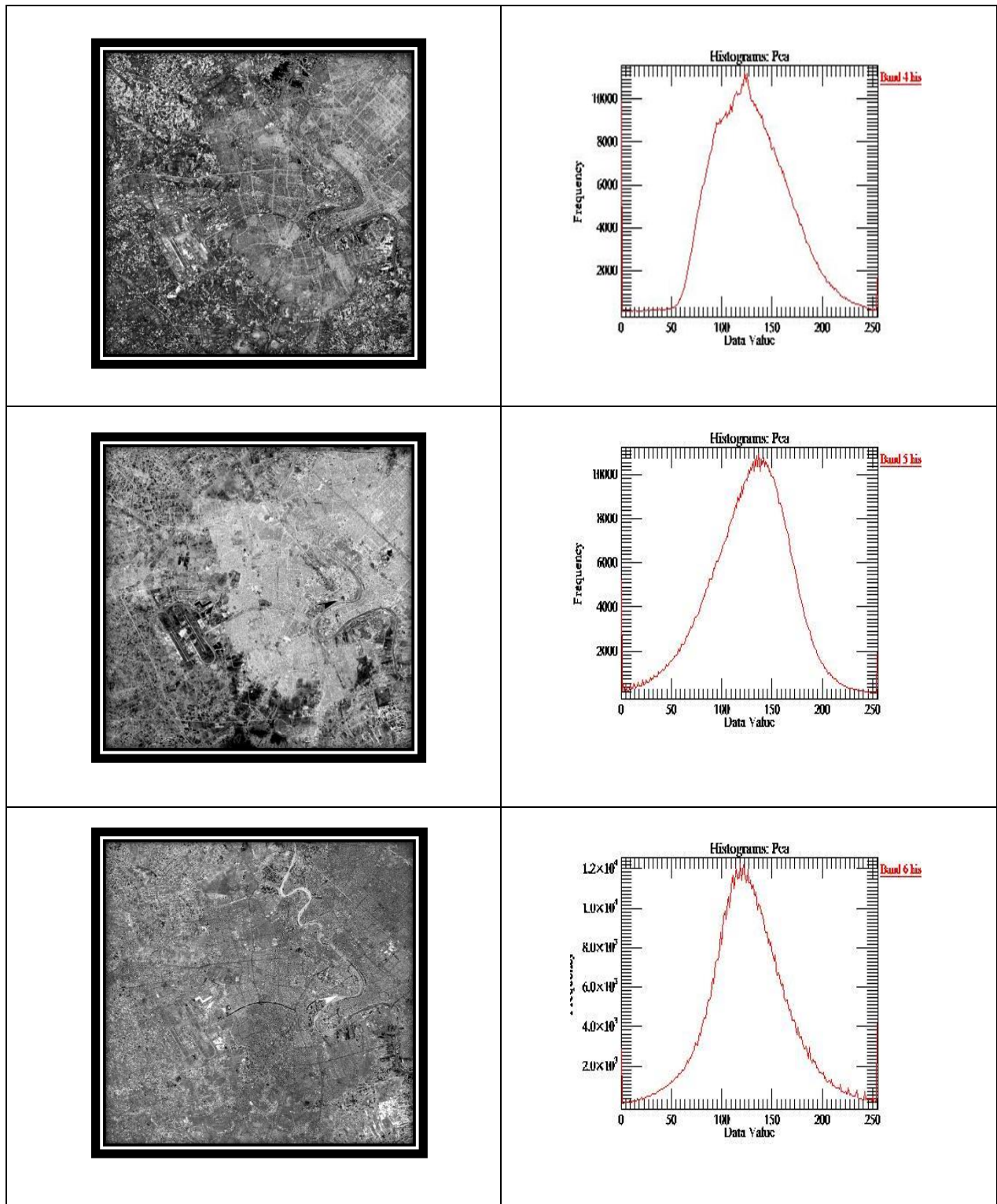| Correlation	pc1	pc2	pc3	pc4	pc5	pc6
pc1	1.00					
pc2	-0.1286	1.00				
pc3	0.0164	0.0162	1.00			
pc4	-0.0544	-0.0125	-0.019	1.00		
pc5	-0.0163	-0.0029	0.0218	-0.0038	1.00	
pc6	0.0146	0.0451	0.0182	-0.0178	-0.0272	1.00
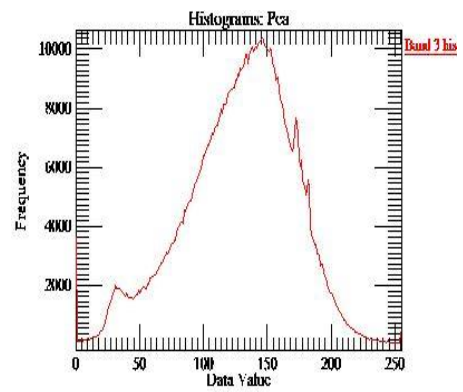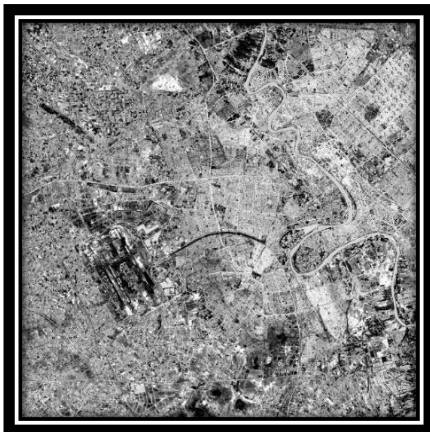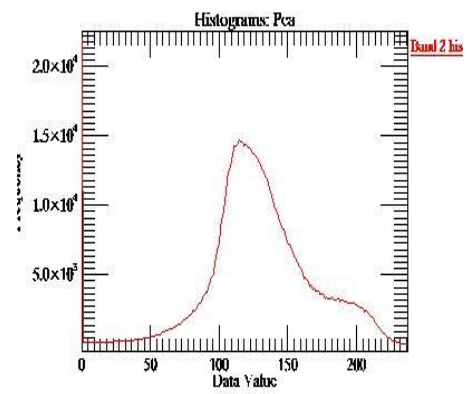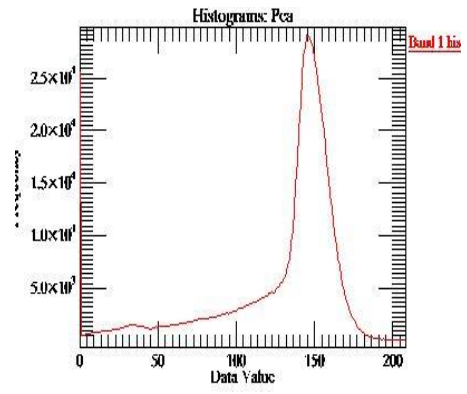
Figure (3-4) The PC's of the scene and the histogram of each PC

Figure (3-5) present the constructed color image by adopting the RGB model for the first two highest Eigenvalues.
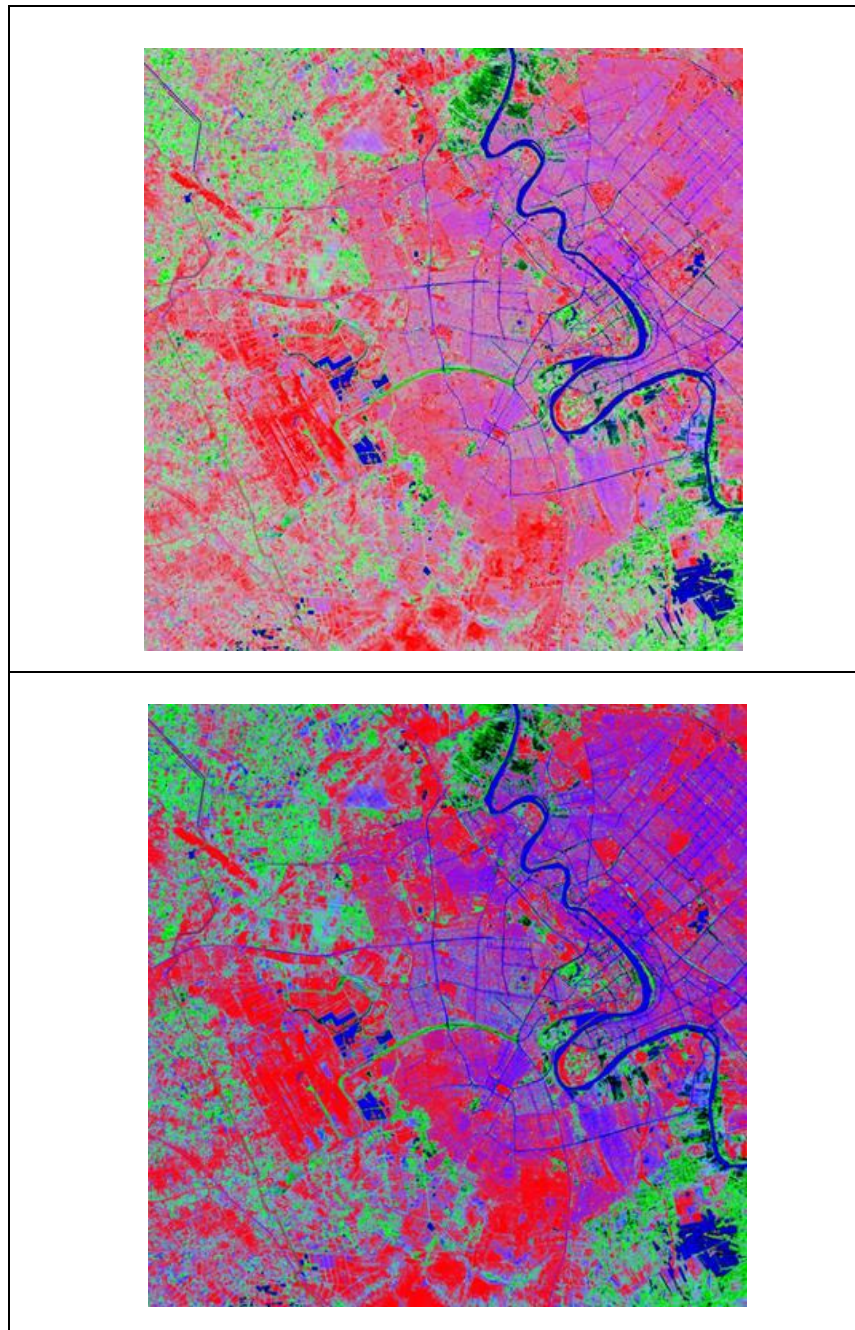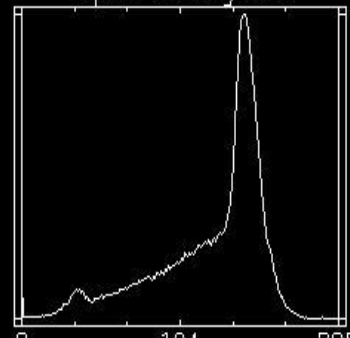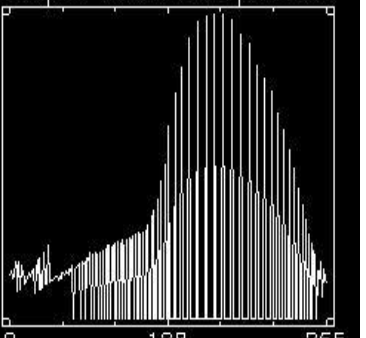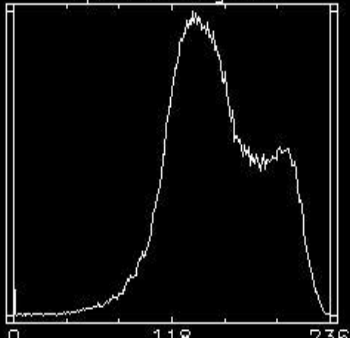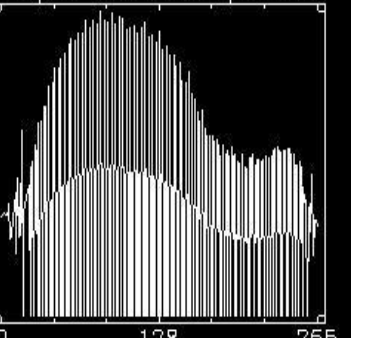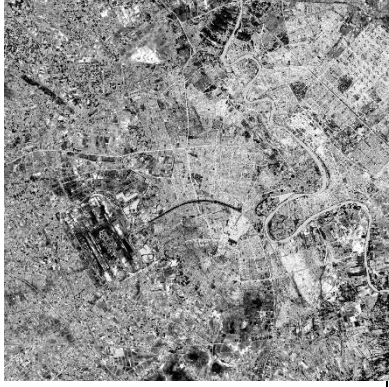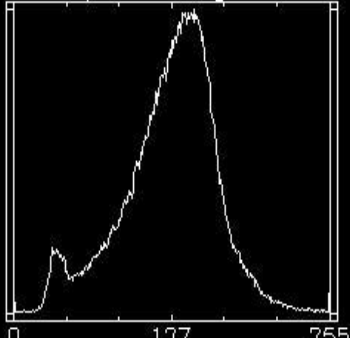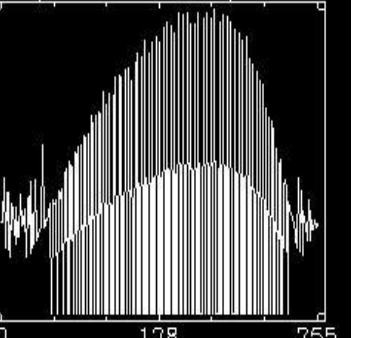
Figure (3-5): Color image of Baghdad scene by adopting the RGB model for the first two highest Eigenvalues.

The final step for enhancing the colored principle component image which is constructed from first three principal component images (the largest sum of eigenvalue), histogram equalization is adopted and applied on each principal component images and The RGB model is applied to these enhanced Principle component images.

Figure (3-6) presents the enhanced images and its histogram for each principal component image. These principle component images became more clarity visually

Figure (3-7) present the final color image which is constructed from the principle component images after applying the histogram equalization technique.

It is clear from the final color image the most of the classes i in the image are clear and distinguished, and it's easy can be select theses classes and calculate the information's for these to build the lookup table for region of interest which is the important step for preparing and applied the maximum likelihood unsupervised classification.

PC 1		
PC 2		
PC 3		

PC 4		
PC 5		
PC 6		

Figure (3-6) Principle component images after applying histogram equalization and their histogram.
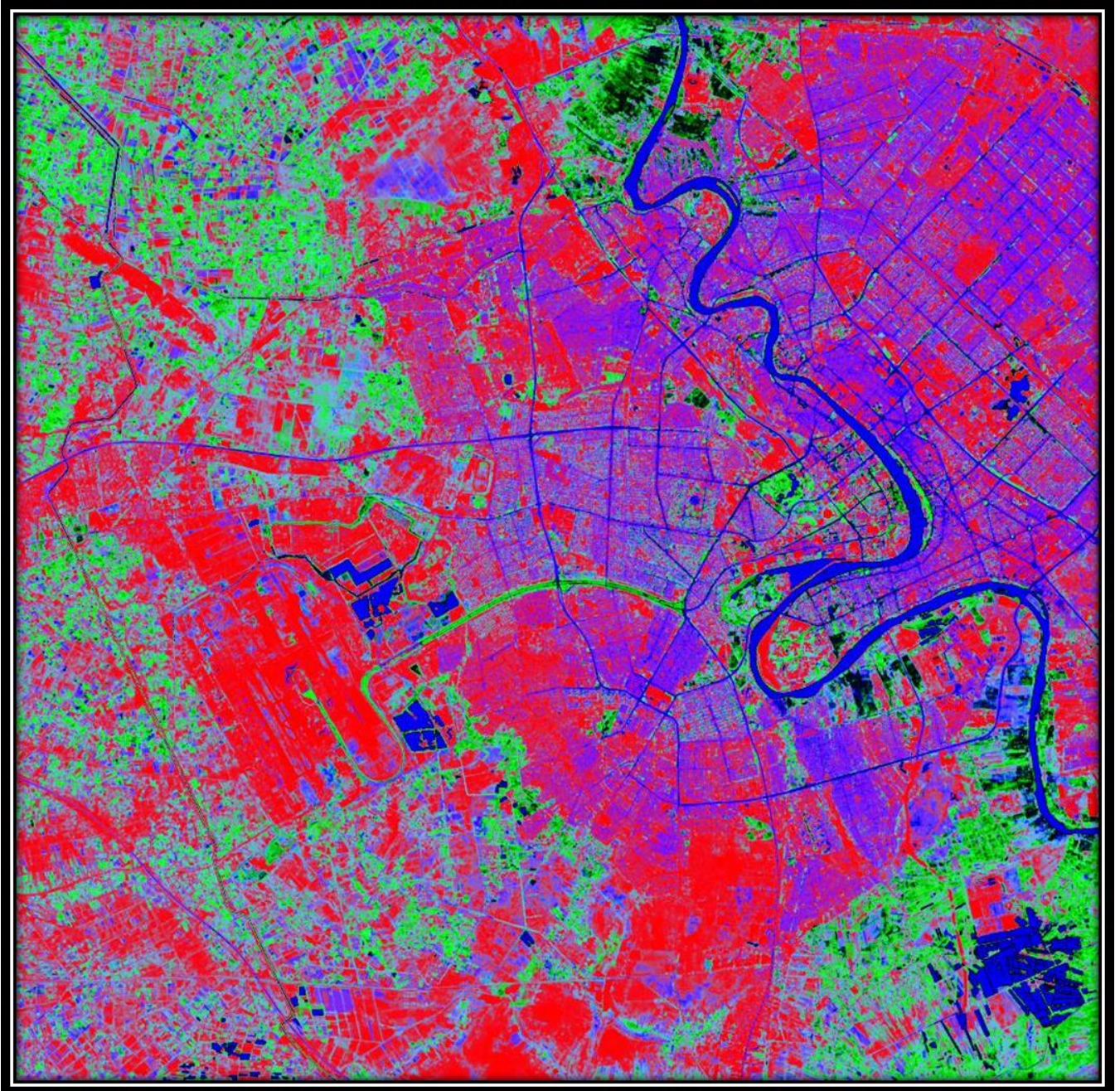
Figure (3-7) Color image of Baghdad scene constructed from enhanced principal component images using RGB model.

3-5   Region of Interest:

When talking about classes, we need to distinguish between **information classes and spectral classes**. Information classes are those categories of interest that the analyst is actually trying to identify in the imagery, such as different kinds of crops, different forest types or tree species, different geologic units or rock types, etc. Spectral classes are groups of pixels that are uniform (or near-similar) with respect to their brightness values in the different spectral channels of the data. The objective is

to match the spectral classes in the data to the information classes of interest. Rarely is there a simple one-to-one match between these two types of classes. Rather, unique spectral classes may appear which do not necessarily correspond to any information class of particular use or interest to the analyst. Alternatively, a broad information class (e.g. Forest) may contain a number of spectral **sub-classes** with unique spectral variations. Using the forest types example, spectral sub-classes may be due to variations in age, species, and density, or perhaps, as a result of shadowing or variations in scene illumination. It is the analyst's job to decide on the utility of the different spectral classes and their correspondence to useful information classes.

In the taken Baghdad scene seven classes were adopted which represent distinguishable classes and used to classify this scene using the maximum likelihood supervised method. These classes chosen from figure (3-7) and projected on one of the original bands as can be seen in figure (3-8).

By returning to spectral reflectance of the original bands for these classes with the aid of the Iraqi Geological Survey organization these classes assigned to the real pattern on the earth as can be seen in table (3-8). The list of these classes are Deep Water, Population, Trees, River, Streets, and various lands (Harvested lands, Barren Lands, Herbals Lands).
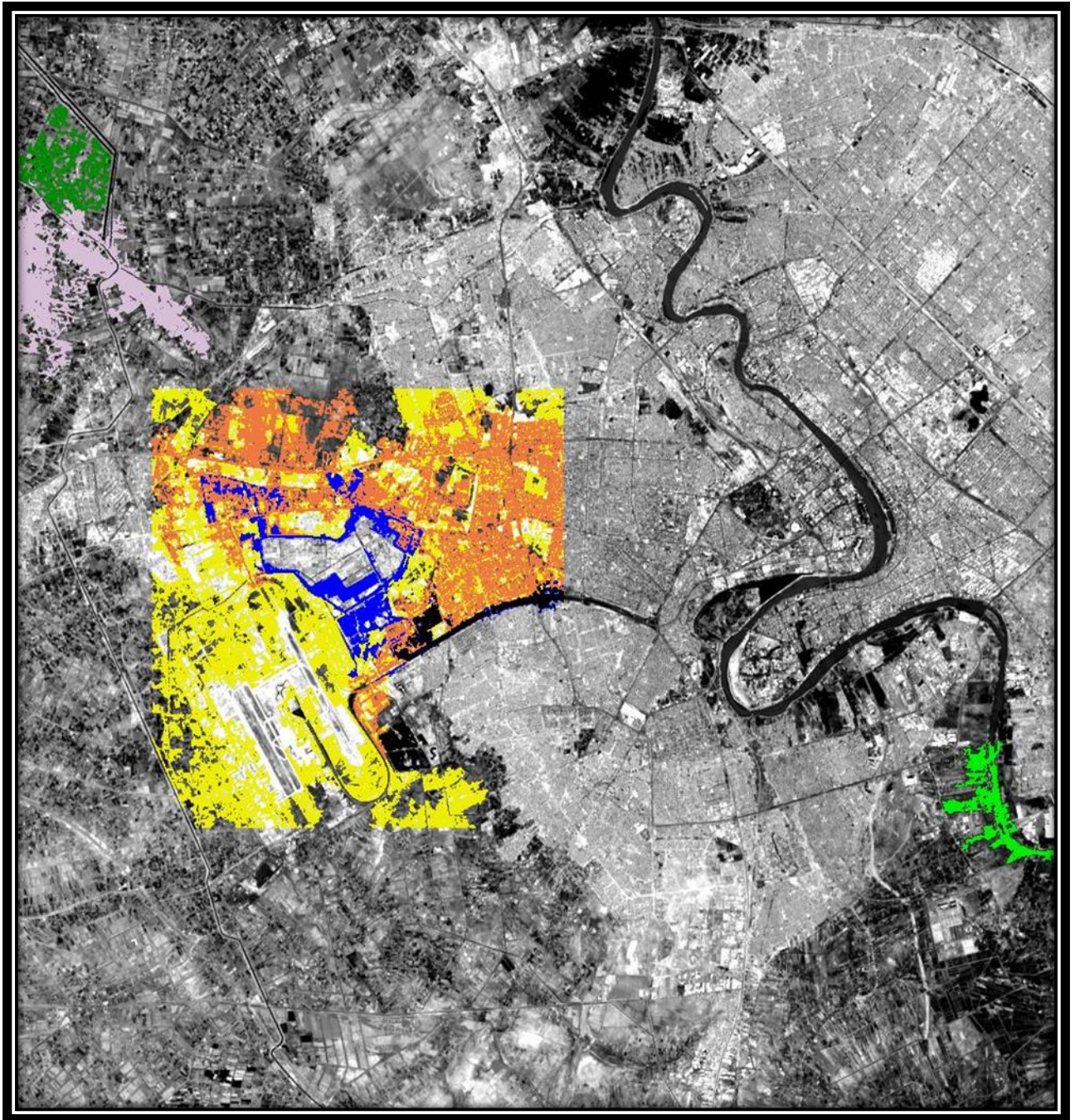
Figure (3-8) show the seven selected regions (ROI) as training classes for Baghdad scene.

Class 1	Class 2	Class 3	Class 4	Class 5	Class 6	Class 7
🟦	🟩	🟧	🟩	⬛	🟪	🟨

Table (3-8) the selected classes labeled relative to the real word classes on the earth

Class1	Class2	Class3	Class4	Class5	Class6	Class7
Deep Water	Harvested Lands	Population	Trees	River And Streets	Barren Lands	Herbals Lands
■	■	■	■	■	■	■

Table (3-9), (3-10), (3-11), (3-12), (3-13), (3-14) and (3-15) represent some of the statistical features computed for six bands which cover each ROI (minimum and maximum value, mean, standard deviation, covariance and correlation matrix).

A. Barren Land:

Table (3-9a) the min., max., standard deviation and the value range of Barren Land scene

Basic Stats	Min	Max	Mean	Stdev	Range
Band 1	164	178	171.49	4.24	14
Band 2	54	95	72.79	11.81	41
Band 3	22	77	47.76	15.71	55
Band 4	136	193	162.43	12.98	57
Band 5	14	173	95.67	24.33	159
Band 7	48	255	126.96	21.73	207

Table (3-9b) the univariate statistics for Barren land scene composed of six bands

Covariance	Band 1	Band 2	Band 3	Band 4	Band 5	Band 7
Band 1	17.97					
Band 2	-49.92	139.45				
Band 3	-66.35	185.34	246.79			
Band 4	53.63	-149.08	-196.8	168.54		
Band 5	-32.86	96.44	139.39	-34.49	591.84	
Band 7	20.66	-58.85	-82.94	34.62	-258.85	472.18

Table (3-9c) correlation between six bands of the Barren Land scene

Correlation	Band 1	Band 2	Band 3	Band 4	Band 5	Band 7
Band 1	1.00					
Band 2	-0.9973	1.00				
Band 3	-0.9965	0.9991	1.00			
Band 4	0.9745	-0.9725	-0.965	1.00		
Band 5	-0.3187	0.3357	0.3647	-0.1092	1.00	
Band 7	0.2243	-0.2294	-0.2430	0.1227	-0.4897	1.00

B. Trees:

Table (3-10a) the min., max., standard deviation and the value range of Trees scene

Basic Stats	Min	Max	Mean	Stdev	Range
Band 1	59	82	69.33	8.12	23
Band 2	6	33	17	9.45	27
Band 3	0	13	1.67	4.30	13
Band 4	196	255	220	23.34	59
Band 5	127	213	172	32.83	86
Band 7	0	121	45	45.58	121

Table (3-10b) the univariate statistics for Trees scene composed of six bands

Covariance	Band 1	Band 2	Band 3	Band 4	Band 5	Band 7
Band 1	192.05					
Band 2	128.99	218.17				
Band 3	250.64	142.55	353.16			
Band 4	535.75	710.5	601.24	2965.97		
Band 5	19.34	-402.94	15.83	-852.98	1763.81	
Band 7	128.68	-116.48	175.75	-102.39	623.5	1537.94

Table (3-10c) correlation between six bands in Trees scene

Correlation	Band 1	Band 2	Band 3	Band 4	Band 5	Band 7
Band 1	1.00					
Band 2	0.6301	1.00				
Band 3	0.9624	0.5136	1.00			
Band 4	0.7099	0.8833	0.5875	1.00		
Band 5	0.0332	-0.6496	0.0198	-0.3729	1.00	
Band 7	0.2368	-0.2011	0.2385	-0.0479	0.3786	1.00

C. Deep Water:

Table (3-11a) the min., max., standard deviation and the value range of a Deep Water scene

Basic Stats	Min	Max	Mean	Stdev	Range
Band 1	0	119	9.92	34.35	119
Band 2	0	131	12	37.66	131
Band 3	128	183	176.83	15.87	55
Band 4	82	203	102.92	31.81	121
Band 5	0	145	23.5	47.94	145
Band 7	97	255	210.5	48.87	158

Table (3-11b) the univariate statistics for Deep Water scene composed of six bands

Covariance	Band 1	Band 2	Band 3	Band 4	Band 5	Band 7
Band 1	1180.08					
Band 2	1287.36	1418.36				
Band 3	-84.74	-151	251.97			
Band 4	1082.72	1167.18	-20.38	1011.72		
Band 5	849.23	1078.46	-701.5	637.77	2298.64	
Band 7	-730.23	-938	658.36	-575.14	-2182.82	2388.64

Table (3-11c) correlation between six bands in the Deep Water scene

Correlation	Band 1	Band 2	Band 3	Band 4	Band 5	Band 7
Band 1	1.00					
Band 2	0.995	1.00				
Band 3	-0.1554	-0.2526	1.00			
Band 4	0.9909	0.9744	-0.0404	1.00		
Band 5	0.5156	0.5973	-0.9217	0.4182	1.00	
Band 7	-0.4349	-0.5096	0.8486	-0.37	-0.9316	1.00

D. Herbals Land:

Table (3-12a) the min., max., standard deviation and the value range of the Herbals Land scene

Basic Stats	Min	Max	Mean	Stdev	Range
Band 1	155	163	158.89	2.38	8
Band 2	95	119	108.15	6.62	24
Band 3	77	110	94.77	8.92	33
Band 4	111	144	125.12	7.53	33
Band 5	72	192	124.23	29.03	120
Band 7	67	209	127.90	29.42	142

Table (3-12b) the univariate statistics for Herbals Land scene composed of six bands

Covariance	Band 1	Band 2	Band 3	Band 4	Band 5	Band 7
Band 1	5.67					
Band 2	-15.59	43.78				
Band 3	-20.93	58.82	79.55			
Band 4	15.99	-43.55	-56.80	56.73		
Band 5	-16.66	56.38	89.80	44.82	842.53	
Band 7	-0.17	1.25	-1.65	0.19	11.81	865.74

Table (3-12c) correlation between six bands in the Herbals Land scene

Correlation	Band 1	Band 2	Band 3	Band 4	Band 5	Band 7
Band 1	1.00					
Band 2	-0.9893	1.00				
Band 3	-0.9852	0.9967	1.00			
Band 4	0.8916	-0.8738	-0.8454	1.00		
Band 5	-0.241	0.2935	0.3469	0.2050	1.00	
Band 7	-0.0024	0.0064	-0.0063	0.0009	0.0138	1.00

E. River and Streets:

Table (3-13a) the min., max., standard deviation and the value range for River and Street scene

Basic Stats	Min	Max	Mean	Stdev	Range
Band 1	45	68	56.60	6.53	23
Band 2	95	164	114.50	14.45	69
Band 3	122	222	186.43	26.90	100
Band 4	198	255	248.53	14.15	57
Band 5	0	110	26.83	29.62	110
Band 7	13	148	48.83	28.12	135

Table (3-13b) the univariate statistics for River and Streets scene composed of six bands

Covariance	Band 1	Band 2	Band 3	Band 4	Band 5	Band 7
Band 1	42.66					
Band 2	-1.31	208.81				
Band 3	93.90	-323.91	723.36			
Band 4	26.67	-110.31	271.28	200.12		
Band 5	-40.62	342.19	-692.93	-365.70	877.39	
Band 7	67.48	309.64	-349.86	-120.74	493.56	789.94

Table (3-13c) correlation between six bands for River and Streets scene

Correlation	Band 1	Band 2	Band 3	Band 4	Band 5	Band 7
Band 1	1.00					
Band 2	-0.0140	1.00				
Band 3	0.5346	-0.8340	1.00			
Band 4	0.2886	-0.5400	0.7130	1.00		
Band 5	-0.2100	0.7995	-0.8700	-0.8730	1.00	
Band 7	0.3676	0.7624	-0.4630	-0.3040	0.5929	1.00

F. Population:

Table (3-14a) the min., max., standard deviation and the value range of Population scene

Basic Stats	Min	Max	Mean	Stdev	Range
Band 1	142	155	148.8	3.39	13
Band 2	119	143	132.13	7.77	24
Band 3	108	146	130.27	11.65	38
Band 4	85	109	95.80	8.67	24
Band 5	80	101	91.60	7.90	21
Band 7	102	165	127.47	16.80	63

Table (3-14b) the univariate statistics for Population scene composed of six bands

Covariance	Band 1	Band 2	Band 3	Band 4	Band 5	Band 7
Band 1	11.46					
Band 2	-24.33	60.41				
Band 3	-38.44	82.68	135.64			
Band 4	20.67	-61.61	-74.37	75.17		
Band 5	0.91	-8.44	-13.24	22.34	62.40	
Band 7	40.81	-110.2	-137.10	126.53	38.91	282.12

Table (3-14c) correlation between six bands in Population scene

Correlation	Band 1	Band 2	Band 3	Band 4	Band 5	Band 7
Band 1	1.00					
Band 2	-0.9250	1.00				
Band 3	-0.9750	0.9134	1.00			
Band 4	0.7044	-0.9140	-0.7370	1.00		
Band 5	0.0342	-0.1380	-0.1440	0.3262	1.00	
Band 7	0.7179	-0.844	-0.7010	0.8685	0.2933	1.00

G. Harvested Land:

Table (3-15a) the min., max., standard deviation and the value range of a Harvested Land scene

Basic Stats	Min	Max	Mean	Stdev	Range
Band 1	2	20	11.72	5.04	18
Band 2	82	163	122.48	20.26	81
Band 3	14	112	59.97	22.85	98
Band 4	0	255	41.80	59.43	255
Band 5	0	236	105.07	39.32	236
Band 7	17	181	113.78	34.90	164

Table (3-15b) the univariate statistics for Harvested Land scene composed of six bands

Covariance	Band 1	Band 2	Band 3	Band 4	Band 5	Band 7
Band 1	25.41					
Band 2	90.49	410.31				
Band 3	-37.95	-332.20	521.93			
Band 4	73.89	-240.40	1051.02	3532.40		
Band 5	-16.80	243.41	-759.02	-1909.57	1546.30	
Band 7	-64.64	-42.91	-216.90	-1167.84	151.18	1218.30

Table (3-15c) correlation between six bands in the Harvested Land scene

Correlation	Band 1	Band 2	Band 3	Band 4	Band 5	Band 7
Band 1	1.00					
Band 2	0.8862	1.00				
Band 3	-0.3295	-0.7179	1.00			
Band 4	0.2466	-0.1997	0.7741	1.00		
Band 5	-0.0848	0.3056	-0.8449	-0.8171	1.00	
Band 7	-0.3674	-0.0607	-0.2720	-0.5630	0.1102	1.00

3-5-1 Supervised Classification Process:

The supervised classification process represents the last step for achieving the aim of our work after performing all the applied processing methods (coloring, histogram equalization, and principal component analysis) to improve the selection of the training area visually clearer and more accurate. As we know, the selection of training areas (regions of interest) plays an important role in supervised classification accuracy. To study the effect of selection of a region of interest on classification accuracy, maximum likelihood method is applied after each executing adopted method since the region of interest is selected at each stage of the adopted applied method.

In this section, we present the results of supervised classification using maximum likelihood method in most cases which the region of interest is chosen in each processing stage. The presented results started by applying maximum likelihood method to the original band and to the enhanced color image and the principal component images. It should be mentioned that the process of classification applied to the original bands except the case where the classification method is directly applied to principal component images.

Figure (3-9) presents the result of supervised classification for the original bands of Baghdad scene. The regions of interest are chosen visually for Baghdad scene. The result showed that the total accuracy is about 85.84% of the seven training samples selected from the original bands

Figure (3-10) presents the result of supervised classification for the original bands of Baghdad scene. The regions of interest are chosen for Baghdad scene after applying the RGB model to the bands which have the largest variance value (bands 7, 5, 3, sum of variance = 10337.8).

Figure (3-9) shows the resulting of the supervised classification for Baghdad scene. The regions of interest are chosen visually for Baghdad scene. The overall accuracy is about (85.84%)
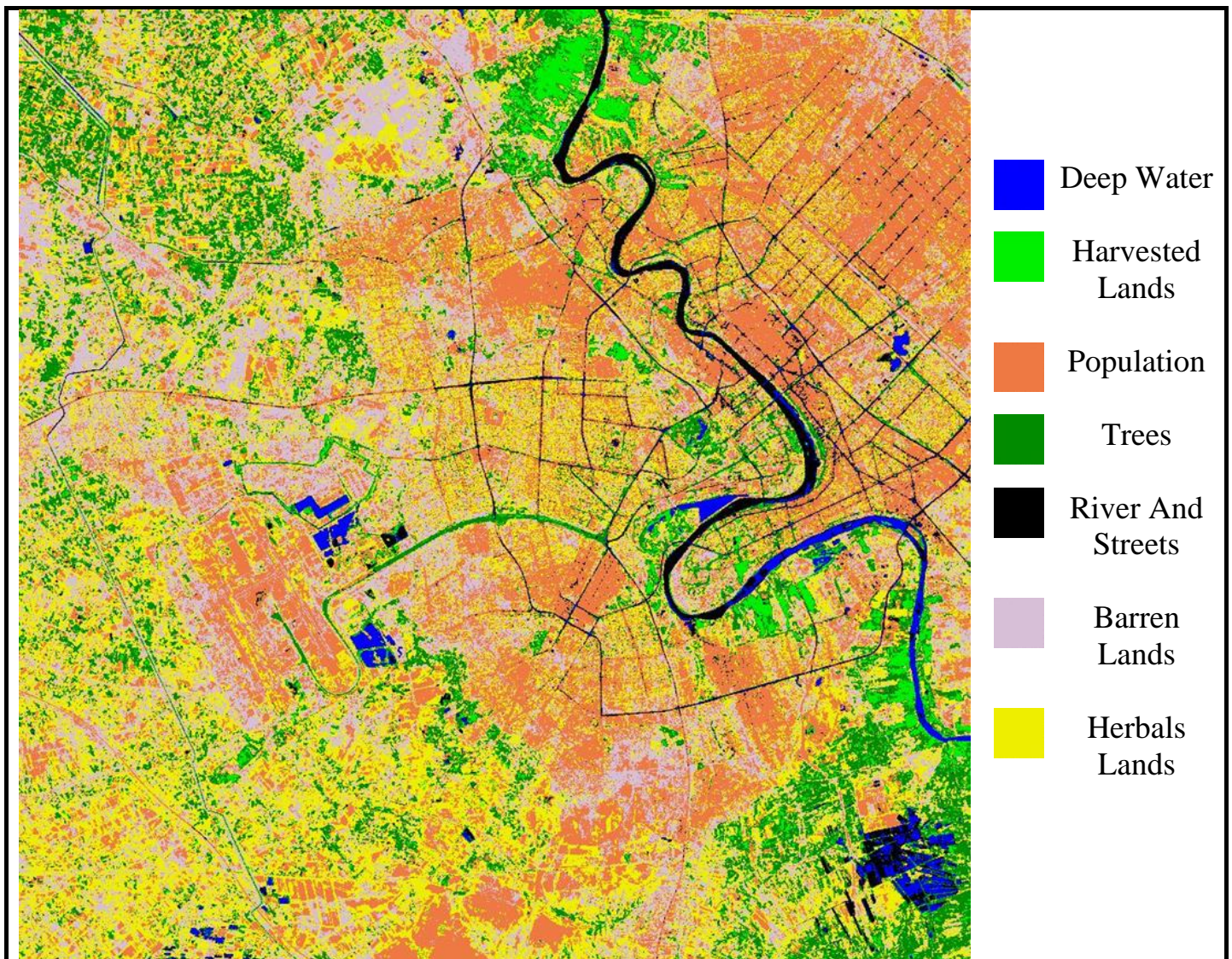
Figure (3-10) shows the result of the supervised classification for Baghdad scene using the six original bands after applying the RGB model to the bands which have the largest variance value (bands 7, 5, 3). The overall accuracy is about (90.13%)

The result showed that the total accuracy is about 90.13% of the seven training samples selected from the original bands.

Table (3-16) represent an error matrix for seven classes after applying histogram equalization on the RGB model to the bands which have the largest variance value (bands 7, 5, 3). The rows elements of the matrix (i, j) represent the number of pixels which have been recognized as to belong to either class i or j. While elements in the principle diagonal line of the table refer to those pixels which were correctly recognized as a member of class i.

The classification accuracy for class (i) is determined from the number of pixels in a cell (i, j) divided by the total number of pixels recognized as to belong to class (i).

Figure (3-11) presents the result of supervised classification for the original bands of Baghdad scene. The regions of interest are chosen for Baghdad scene after applying histogram equalization on the RGB model to the bands which have the largest variance value (bands 7, 5, 3). The result showed that the overall accuracy is about 97.08% of the seven training samples selected from the original bands. The overall accuracy is computed by averaging theses accuracy values in column B in table (3-16).

Table (3-17) shows the percentage of each class in the scene. It's clear from this table that dominant area in the scene is population 36.5%, while the water not more than 0.7%
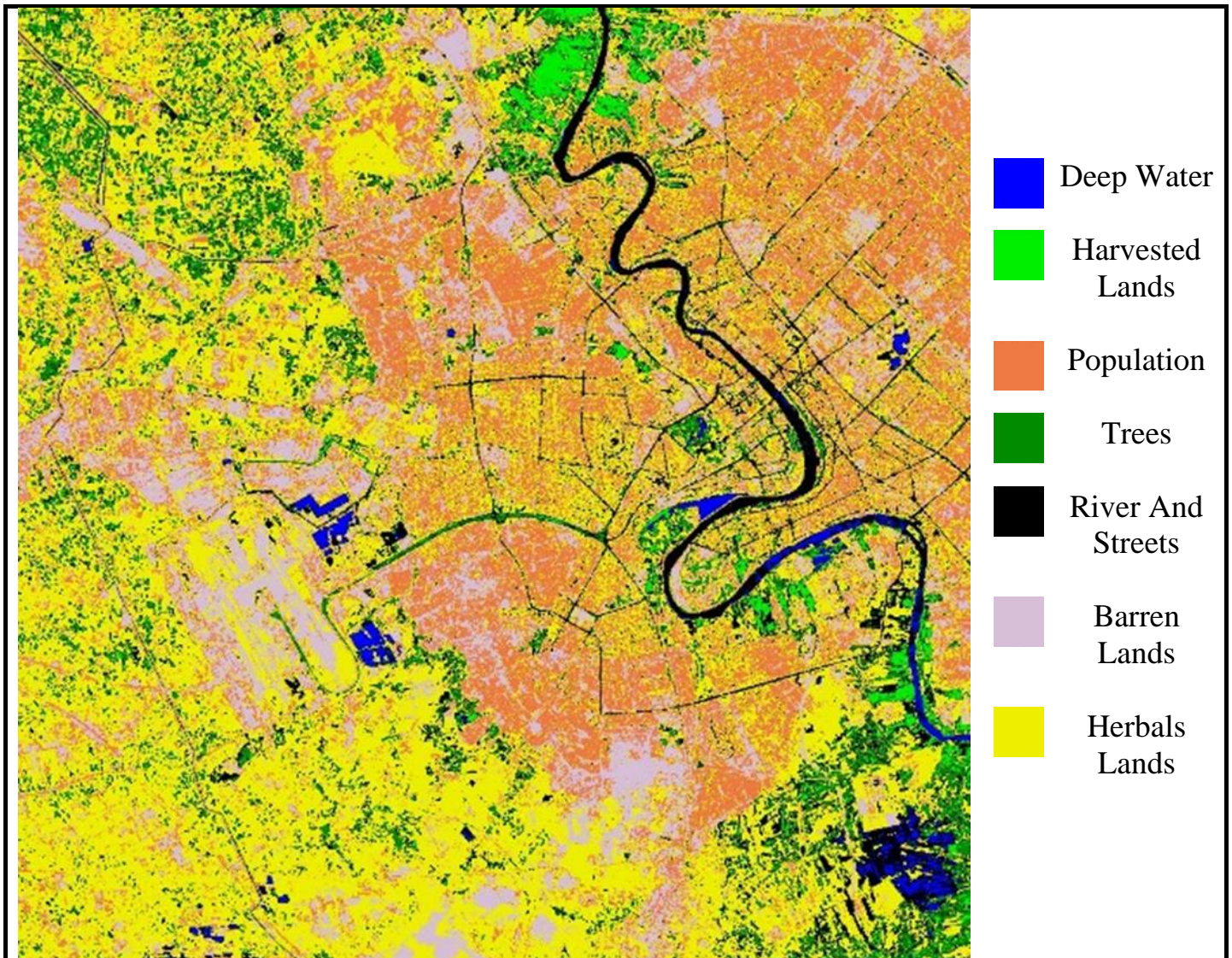
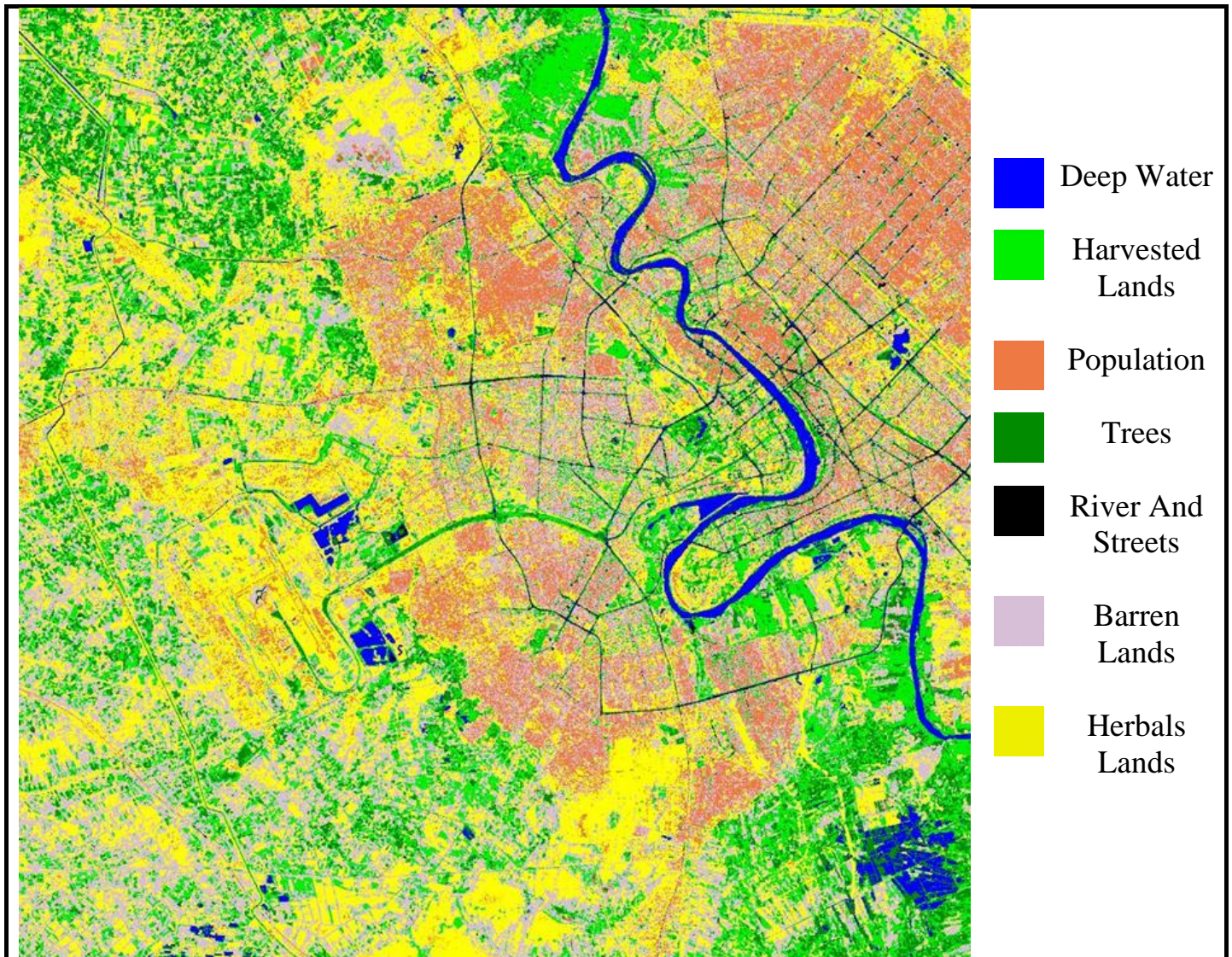**Figure (3-11) The result of the supervised classification for Baghdad scene. The regions of interest are chosen after applying histogram equalization on the RGB model to the bands which have the largest variance value (bands 7, -5, 3). The overall accuracy is about (97.08%).**

Table (3-16) Error matrix for seven classes after applying histogram equalization on the RGB model to the bands which have the largest variance value (7, 5, 3)

Classes	Barren Land	Trees	Deep water	Herbals Lands	Streets	Population	Harvested Land	A	B%	C	D
Barren Land	387	0	0	7	0	0	0	394	98.22	7	9
Trees	0	312	0	6	0	0	4	322	96.89	10	7
Deep Water	0	0	224	0	1	0	0	225	99.56	1	0
Herbals Land	9	0	0	272	0	5	0	286	95.11	14	26
River and Streets	0	0	0	0	352	6	2	360	97.78	8	1
Population	0	0	0	2	0	372	3	377	98.67	5	11
Harvested Land	0	7	0	11	0	0	252	270	93.33	18	9
								2234		63	63

A: the number of the pixels in classes

B: the classification accuracy for each class (percentage)

C: the classified pixels in reflectance data with incorrect label

D: pixel labeled with incorrect class in reflectance data

The overall accuracy = 97.08%

Table (3-17) the percentage of each class in the scene (97.08%)

Class type	Barren Land	Trees	Deep Water	Herbals Land	River and Streets	Population	Harvested Land
Class number	1	2	3	4	5	6	7
No. of pixels in each class	76742	113295	6731	334459	80435	362591	17714
Percentage of each class type%	7.74%	11.42%	0.68%	33.72%	8.11%	36.55%	1.79%

Figure (3-12) presents the result of supervised classification for the principal component images of Baghdad scene. The regions of interest are selected from the color image of Baghdad scene constructed from the first three principal component images using the RGB model figure (3-7).

The result showed that the overall accuracy is about 98.74% of the seven training samples selected from the principle components. The overall accuracy is computed by averaging theses accuracy values in column B in table (3-18).

Table (3-19) shows the percentage of each class in the scene. It's clear from this table that dominant area in the scene is population 39.92%, while the water not more than 0.40%.

It should be mentioned that all this information in table (3-19) are time dependent, because of the changes in the nature of the land cover from a certain time to another.

Table (3-20) summarize the results of the overall accuracy in supervised classification (maximum likelihood method) for all cases, which have been adopted in this study.
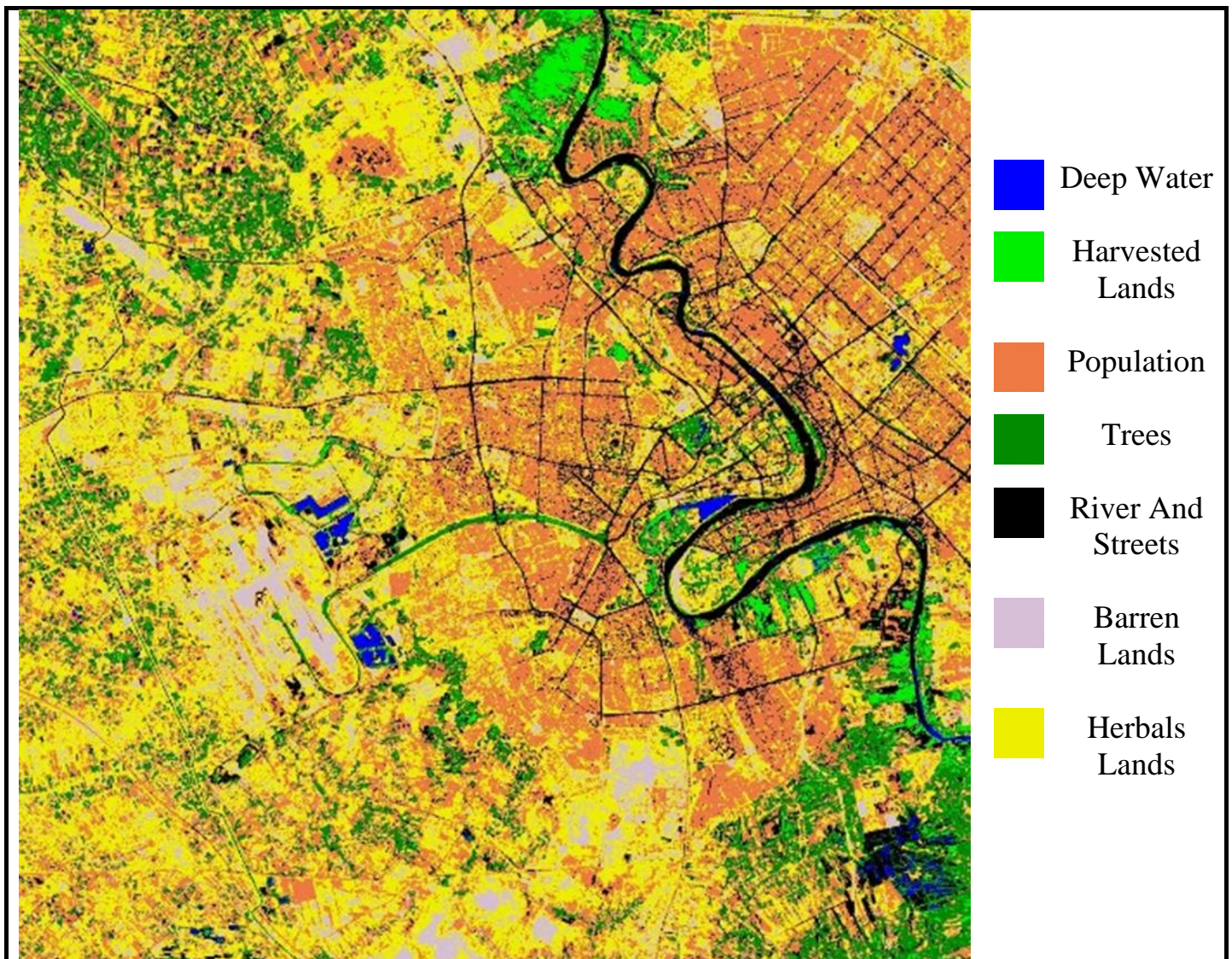
Figure (3-12) shows the resulting of the supervised classification for Baghdad state scene using the six original bands (overall accuracy PC's (98.86%)).

Table (3-18) Error matrix for seven classes after on the RGB model to the Principle Components

Classes	Barren Land	Trees	Deep water	Herbals Lands	Streets	Population	Harvested Land	A	B%	C	D
Barren Land	387	0	0	7	0	0	0	394	98.22	7	1
Trees	0	322	0	0	0	0	0	322	100	0	3
Deep Water	0	0	224	0	1	0	0	225	99.56	1	2
Herbals Land	1	1	0	284	0	0	0	286	99.30	2	12
River and Streets	0	0	1	0	353	4	2	360	98.06	7	2
Population	0	0	0	2	0	372	3	377	98.67	5	4
Harvested Land	0	2	1	3	1	0	263	270	97.41	7	5
								2234		29	29

A: the number of the pixels in classes

B: the classification accuracy for each class (percentage)

C: the classified pixels in reflectance data with incorrect label

D: pixel labeled with incorrect class in reflectance data

The overall accuracy = 98.74%

Table (3-19) the percentage of each class in the scene (98.74%)

Class type	Barren Land	Trees	Deep Water	Herbals Land	River and Streets	Population	Harvested Land
Class number	1	2	3	4	5	6	7
No. of pixels in each class	56964	173659	3981	231440	114692	395936	15295
Percentage of each class type%	5.74%	17.51%	0.40%	23.33%	11.56%	39.92%	1.54%

Table (3-20) the results of the overall accuracy in supervised classification (maximum likelihood method) for all cases, which have been adopted in this study

No	Type of bands or components		Selected bands or components	Overall accuracy
1	Principal component		(1,2,3)	98.86%
			(1,2,3,4)	98.96%
			(1,2,3,4,5)	98.86%
			(1,2,3,4,5,6)	98.74%
2	Original bands	Visually	(1,2,4)	90.34%
			(1,2,4,5)	89.14%
			(1,2,3,4,5)	90.03%
			(1,2,3,4,5,7)	90.13%
		Statistics	(7,5,3)	74.28%
			(7,5,3,4)	68.54%
			(7,5,3,4,2)	82.89%
			(7,5,3,4,2)	90.13%
3	Enhanced original bands with histogram equalization		(7,5,3)	82.41%
			(7,5,3,4)	79.65%
			(7,5,3,4,2)	89.33%
			(7,5,3,4,2)	97.08%

CHAPTER FOUR

Conclusions and Recommendations

This chapter is dedicated to summarize and gives the main conclusions that derived from the present work in addition to the recommendations work for the future.

4-1 Conclusions:

This work aimed to classify multi-spectral satellite images using the original image bands (row data) and principal component images for the taken Baghdad scene. The problem of this study focused on the effect of the selecting of the training area (region of interest) on the accuracy of the classification process. From the result of this study one can conclude the following remarks.

1. The image with a higher variance value doesn't represent a prerequisite in image clarity. The variance with mean value may reflect the quality of the image. The variance and means look like the torque in physics. So that we can see that the image with low variance and mean value near the middle of the dynamic range value has more quality than the image with high variance and mean value near the edgce of the minimum or maximum value.

2. Improving the selection of the training area (region of interest) visually plays an essential role in increasing the accuracy of supervised classification and this reflects on the calculation of the area for each class in the scene. In the present work, the overall accuracy increased from 68.5% to 98.9% (see table (3-20)) after adopting the histogram equalization technique as an enhancement technique in improving the selecting the training area visually.

3. Dealing with principal component images (PC's) solved the problem for choosing of which bands are the best for classification purpose. This is so because the principal component images are arranged from the component of high energy (contain most of the details, the first principal component image) to the lowest one.

4. The result of classification accuracy is very high with principal component image, but still the classification process with original bands becomes better than the one of are dealing with principal component images. By returning to the second conclusion the result of classification accuracy with the original bands is enhanced

from 68.5% to 97.08% and became very comparable with the result of classification accuracy with the principal component images 98.86%.

4-2 Recommendations:

Many suggestions for the future could be possible here for developing the present work, these are:

1. Hybrid method combines between the original spectral bands and principal component image could be chosen with the selecting the type and the number images for classification purpose.

2. There are other color models like YIQ, HSI. These color models can be adopted to build color image to help in selecting the training areas in the images.

3. Another enhancement model like histogram specification can be adopted to enhance the color image to help in selecting the training area in the image.

REFERENCES

5-1 References:

[Afa 96]

Afaf A.S. "Expert System for Classification and Enhancement of Landsat (TM) Images" M.Sc. Thesis, University of Baghdad, College of Science, 1996.

[Ahm 97]

Ahmed A.K. "Automatic Change Detection Using Digital Satellite Images", M.Sc. Thesis, Saddam University, College of Science, 1997.

[Al-Ahm: 09]

Ahmadi F. S. Al- and Hames A. S., "Comparison of Four Classification Methods to Extract Land Use and Land Cover from Raw Satellite Images for Some Remote Arid Areas, Kingdom of Saudi Arabia", Journal of King Abdul Aziz University, Earth Sciences, Vol: 20, Issue 1, pp167 -191, 2009.

[Aly 98]

Alyaa H. H., "Studying the Flooded Area by Principal Component Analysis of Multi-Temporal Landsat Thematic Mapper Data", M. Sc. Thesis Saddam University, College of Science, 1998.

[Arj 01]

Arjen V. O. "New Approach for the Generation and Analysis of Microbial Typing Data", PP. 31-45, 2001.

[Asm 12]

Asmala A., "Analysis of Maximum Likelihood Classification on Multispectral Data", Applied Mathematical Sciences, Vol. 6, pp 6425 – 6436, 2012

[Ban 97]

Ban A. A., "Aerial Image Regions Classification" M.Sc. Thesis, University of Baghdad, College of Science, 1997.

[Bal 13]

Balaji T., Sumathi M., "Relational Features of Remote Sensing Image classification using Effective K-Means Clustering", International Journal of Advancements in Research & Technology, Vol 2, Issue 8, pp 103-107, 2013.

[Bla 10]

Blaschke T. "Object based image analysis for remote sensing", ISPRS Journal of Photogrammetry and Remote Sensing, Vol 65, pp 2–16, 2010

[Byr 80]

Byrne G. F., "Monitoring Land-Cover Change by PCA of Multi-temporal Landsat Data" Remote Sensing of Environment, Vol.10, PP.175-184., 1980.

[Car 13]

Carlos H., Erivelto M., Victor H., and Diego J., "Methods of performance evaluation for the supervised classification of satellite imagery in determining land cover classes", Ciencia E Investigación Agraria, Vol 40, pp 419-428, 2013.

[Cha 89]

Chavez P.S. Jr. "Extracting Spectral Contrast in Land sat Thematic Mapper Image Data Using Selective PCA", Photogrammetric Engineering and Remote Sensing, Vol.55, No.3, PP.339-348, 1989.

[Chr 13]

Christopher E. N., Segun M. O., Inemesit M. A., "Supervised Learning Methods in the Mapping of Built Up Areas from Landsat-Based Satellite Imagery in Part of Uyo Metropolis", New York Science Journal, Vol 6, No.9, pp 45-52, 2013.

[Cla 03]

Clarke, K. C. "Getting Started with Geographic Information Systems", Fourth Edition, Prentice Hall, Upper Saddle River, NJ. 2003

[Dav 15]

David C., "Environmental Science and Information Application Technology", CRC press, 2015

[Ema 01]

Eman F. A. "Satellite Image Processing for "GIS" Application", Ph.D. Thesis, University of Baghdad, College of Science, 2001.

[Eas 01]

Eastman J. R., "Guide to GIS and Image Processing", Clark University, Vol 1, 2001.

[Fun 87]

Fung. F. and Ledreu. E, "Application of PCA to Change Detection", American Society for Photo-Grammetry and Remote Sensing, Vol. 53, No. 12, PP. 1649-1658, 1987.

[Gib 00]

Gibson P. J. &Power C. H., "Introductory Remote Sensing: Digital Image Processing and Application", 1St Published, New York, 2000.

[Gil 11]

Gil, Q. Yu, A. Lobo, P. Lourenço, L. Silva and H. Calado, "Assessing the effectiveness of high resolution satellite imagery for vegetation mapping in small islands protected areas", Journal of Coastal Research, SI 64, pp 1663 – 1667, 2011.

[Gon: 87]

Gonzalez R.C. & Poul W. R., "Digital Image Processing" 2nd Ed., Addison-Wesley Publishing Company, Inc., 1987.

[Gon: 02]

Gonzalez R. C. and Woods R. E., "Digital image processing", 2nd ed. Boston, MA, USA: Prentice-Hall of India, 2002.

[Gon and Woo 08]

Gonzalez R. C. and Woods R. E., "Digital image processing", 3nd ed. Pearson Education, 2008.

[Hai 10]

Hailiang S., "Fusion of multispectral and panchromatic satellite images using Principal Component Analysis and No subsampled Contour let Transform", Fuzzy Systems and Knowledge Discovery (FSKD), 2010 Seventh International Conference, Vol 5, pp 2312 – 2315, 2010

[Har 15]

Harikrishnan R., S. poongodi, "Satellite image classification for IRS data based on supervised and unsupervised algorithms using ERDAS", International Conference on Engineering Trends and Science & Humanities, pp 112-116, 2015.

[Hor 85]

Hord R. M., "Remote Sensing Methods and Application", John Wiley and Son, USA. 1985.

[Hot 33]

Hotelling H. "Analysis of Complex of Statistical Variables into Principal Components", J. Educ. Psychol., vol.24, PP 417-441, 498-520, 1933

[Jen 86]

Jensen J. R. "Introductory Digital Image Processing- A Remote Sensing, Perspective, Printice-Hall, Englewood Cliffs, New Jersey", 1986.

[Jen 04]

Jensen, J. R. "Introductory Digital Image Processing, A Remote Sensing Perspective", 3rd ed., Prentice Hall Series in Geographic Information Science, Prentice-Hall Inc., Upper Saddle River, New Jersey, 2004

[Jen 07]

Jensen J. R. "Remote Sensing of the Environment", Second Edition Pearson Prentice Hall, 2007

[Joh 13]

John A. R., "Remote Sensing Digital Image Analysis: An Introduction", Springer, 2013.

[Juw 08]

Juwairia zubair, "Image Enhancement for Improving Visibility and Feature Recognition", M.Sc. Thesis, University of Texas, 2008.

[Kan 13]

Kanika K., Anil K. G., Rhythm G., "A Comparative Study Of Supervised Image Classification Algorithms For Satellite Images", International Journal of Electrical, Electronics and Data communication, Vol 1, pp 10-16, 2013.

[Kim 97]

Kim Y. T., "Contrast enhancement using brightness preserving bi histogram equalization," IEEE Trans. On Consumer Electronics, Vol. 43, no. 1, pp. 1-8, 1997.

[Lai 96]

Laith A. A. "Classification of Digital Satellite Images", Ph.D. Thesis, Saddam University, College of Science, 1996.

[Lai 11]

Laith A. A., Mohammed S. M., "Multi-Band Image Classification Using KLT and Fractal Classifier", Journal of Al-Nahrain University, Vol.14, pp.171-178, 2011.

[Lai: 13]

Laith A. A., "Image Integration Based Ant Colony System for Multiband Satellite Image Classification", Journal of Al-Nahrain University, Vol.16, pp.129-139, 2013.

[Lee 99]

Leeser M. "K-Mean Algorithm for Unsupervised Classification", WWW.ccrs. nrcan. Gc. Ca/-6k, 1999.

[Lli 00]

Lliesand T. M. & Kiefer R.W., "Remote Sensing and Image Interpretation" 4th Ed., John Wiley and Sons, 2000.

[Lor 01]

Lorenzo B. and Diego F. P., "Unsupervised Retraining of a Maximum Likelihood Classifier for the Analysis of Multitemporal Remote Sensing Images", IEEE TRANSACTIONS ON GEOSCIENCES AND REMOTE SENSING, VOL. 39, NO. 2, pp 456-460, 2001

[Man 13]

Mandeep Kaur, Kiran Jain, Virender Lather, "Study of Image Enhancement Techniques: A Review", International Journal of Advanced Research in Computer Science and Software Engineering, IJARCSSE, Vol. 3, pp. 846 –848, April 2013.

[Man 13]

Manoj P., Astha B., M.B. Potdar, M.H. Kalubarme, Bijendra A., "Comparison of Various Classification Techniques for Satellite Data", International Journal Of Scientific & Engineering Research, Vol 4, Issue 2, pp 1-6 ,2013

[Mar 14]

Maryam N., Vahid M. Z., Mehdi H., "Comparing different classifications of satellite imagery in forest mapping (Case study: Zagros forests in Iran)",

International Research Journal of Applied and Basic Sciences, Vol 8 (7), pp 1407-1415, 2014.

[Mic 86]

Michael R. H., "Remote sensing methods and applications", John Wiley and sons, New York, 1986

[Muc 94]

Muchoney D. M. and Heach B. N., "Change Detection for Monitoring Forest Defoliation", American Society for Photogrammetry and Remote Sensing. Vol. 60, No. 10, PP. 1243-1251, 1994.

[Muk 13]

Mukhtar M.E, Younes D. E., Abdulhakim E. and Farag A. "Performance of Supervised Classification for Mapping Land Cover and Land Use in Jeffara Plain of Libya 2013", International Conference on Food and Agricultural Sciences, IPCBEE vol.55 (2013)

[Neh 12]

Neha Gulati & Ajay Kaushik, "Comparative Analysis of Image Restoration of Remote Sensing Images using Lucy Richardson, Wiener and Blind De-Convolution", Vol. 2, No. 1, 2012.

[Par 14]

Parivallal R., Dr. B. Nagarajan, "Supervised Classification Methods For Object Identification Using Google Map Image", International Journal of Engineering Sciences & Management Research, pp 71-79, 2014.

[Pei 04]

Pei C., Zeng C., and Chang H., "Virtual Restoration of Ancient Chinese Paintings Using Color Contrast Enhancement and Lacuna Texture Synthesis," Computer Journal of IEEE Transactions Image Processing, Vol 13, no. 3, pp. 416-429, 2004.

[Per 10]

Perumal K. and Bhaskaran R., "Supervised Classification Performance of Multispectral Images", Journal of Computing, Vol 2, Issue 2, pp 124-129, 2010

[Piz 03]

Pizer M., "The Medical Image Display and Analysis Group at the University of North Carolina: Reminiscences and Philosophy," Computer Journal of IEEE Transactions on Medical Image, Vol. 22, no.1, pp. 2-10, 2003.

[Pri 14]

Priyanka A., A.N. Khobragade, V.A.Tehre, "Study of Classification Techniques on Multispectral Remote Sensing Data for Agricultural Application", IOSR Journal of Electrical and Electronics Engineering (IOSR-JEEE), ISSN: 2320-3331, pp 76-78, 2014.

[Raj 11]

Rajesh Garg, Bhawna Mittal, Sheetal Garg, "Histogram Equalization Techniques for Image Enhancement," International Journal of Electronics & Communication Technology, IJECT, Vol. 2, pp. 107–111, March 2011.

[Rea 73]

Ready P. J. And Wintz P. A., "Information Extraction, SNR Improvement, and Data Compression in Multi-Spectral Imagery", IEEE Transactions on Communications, Vol. 21, No. 10, PP. 1123-1129, 1973.

[Sab 78]

Sabins F. F. "Remote sensing: Principle and Interpretation", 1978.

[Sab 14]

Sabna S., Ratika P., "Classification Methods for Land use and Land Cover Pattern Analysis", International Journal of Innovative Technology and Exploring Engineering (IJITEE), Vol 4, Issue 1, pp 36-38, 2014.

[San 78]

Alfonso Santisteban, "Principal Component of a Multi-Spectral Image: Application to a Geological Problem", IBM. J. RES, Vol.22, No. 5, 1978.

[Sed 85]

Seddon A. M. And Hunt G. E., "Segmentation of Clouds Using Cluster Analysis", INT. Remote Sensing, Vol.6, No.5, PP. 717-731, 1985.

[Sie , Men 05]

Siegmund, A. & Menz, G., "Fernes nah gebracht – Satelliten- und Luftbildeinsatz zur Analyse von Umweltveränderungen im Geographieunterricht". Geographie und Schule 154, P. 2-10, 2005.

[Sim 62]

Simonds J. L., "Application of Characteristic Vector Analysis to Photographic and Optical Response Data", Journal of the Optical Society of America, Vol.53, No.8, PP. 968-974, 1962.

[Sin 85]

Singh A. And Harrison a., "Standardized Principal Components", INT. J. Remote Sensing. Vol.6, No.6, PP. 883-896, 1985.

[Sub 12]

Subhash T., Akhilesh S., Seema S., "Comparison of Different Image Classification Techniques for Land Use Land Cover Classification: An Application in Jabalpur District of Central India", International Journal of Remote Sensing and GIS, Vol 1, Issue 1, pp 26-31, 2012.

[Sun 15]

Sunitha A., Suresh B. G., "Satellite Image Classification Methods and Techniques: A Review", International Journal of Computer Applications, Vol 119 – No.8, p 20, 2015.

[Swa 78]

Swain P. H. &Davis S. M, "Remote Sensing: The Quantitative Approach", Mc Graw Hill, 1978.

[Tar 10]

Tarun K., Karun V., "A Theory Based on Conversion of RGB image to Gray image", International Journal of Computer Applications, Vol 7– No.2, pp 7-10, 2010.

[Thw 15]

Thwe Z. P., Aung S. K., Hla M. T., "Classification Of Cluster Area For satellite Image", INTERNATIONAL JOURNAL OF SCIENTIFIC & TECHNOLOGY RESEARCH, Vol 4, Issue 6, pp 393-397, 2015.

[Waf 99]

Wafaa K.S. "Adaptive Principal Components Methods for Images Classification and Coding", M. Sc., Thesis, University of Baghdad, College of Science, 1999.

[Wan 99]

Y. Wang, Q. Chen, and B. Zhang, "Image enhancement based on equal area dualistic sub-image histogram equalization method," IEEE Trans. on Consumer Electronics, Vol. 45, no. 1, pp. 68-75, 1999.

[Wei 07]

Wei D. L. and Qihao W., "A survey of image classification methods and techniques for improving classification performance", International Journal of Remote Sensing, Vol. 28, No. 5, pp 823–870, 2007

[Xiu 94]

Xiuping J. and John A. R. "Efficient Maximum Likelihood Classification for Imaging Spectrometer Data Sets", IEEE TRANSACTIONS ON GEOSCIENCE AND REMOTE SENSING, VOL. 32, NO. 2, pp 274-281, 1994.

[Yul 15]

Yulin D., Xiaowei S., Yun S., Hiroyuki M., Koki I. and Ryosuke S., "Unsupervised Global Urban Area Mapping via Automatic Labeling from ASTER and PALSAR Satellite Images", Remote Sens, Vol 7, pp 2171-2192, 2015.

الخلاصة

واحدة من الأهداف الرئيسية لصور الأقمار الصناعية للاستشعار عن بعد هو تفسير البيانات المستقبلة وتصنيف المميزاتها. تصنيف الصور الفضائية يلعب دورا كبيرا في استخراج وتفسير المعلومات القيمة من صور الأقمار الصناعية الضخمة.

والغرض الرئيسي من هذا البحث هو تصنيف صور الأقمار الصناعية متعددة الأطياف (Thematic Mapper) باستخدام التصنيف الموجه. التصنيف الغير موجه (نموذج التلوينRGB) والتصنيف الموجه (طريقة ال maximum likelihood) لتحقيق غرض التصنيف. دقة تصنيف تعتمد على دقة اختيار منطقة التدريب.

التحويل بطريقة ال PCA يتم تبنيها وتطبيقها على الحزم الأصلية لإنشاء الصور ال(principal component). الصور الثلاثة الأولى للتحتوي على معظم المعلومات في جميع الحزم الأصلي. لهذا الغرضيتم اختيار أول ثلاث صور (principal component) كصور RGB لخلق صورة ملونة.

وقد استخدمت هذه الصورة الملونة لتحديد واختيار مناطق التدريب التي هي مهمة جدا لتصنيف الموجه و بعد تطبيق طريقة التحسين ال histogram equalization على الصورة الملونة لزياد في الدقة والوضوح في اختيار منطقة التدريب. و بعد اختيار المناطق التدريب ستكون الصورة مستعدة للتصنيف الموجه.

نتائجنا تظهر ان الصورة مع قيمة التباين العالي لا يمثل شرطا أساسيا في وضوح الصورة. التباين مع القيمة المتوسطة قد يعكس جودة الصورة. التباين و متوسط القيم قد يعكس مبداء عزم الدوران في الفيزياء. بحيث يمكننا أن نرى أن الصورة مع انخفاض التباين ومتوسط القيمة بالقرب من منتصف قيمة النطاق الديناميكي لديه أكثر جودة من الصورة مع التباين العالية ومتوسط القيمة التي تكون بالقرب من قيمة الحافة الأدنى أو الأقصى. تحسين اختيار منطقة التدريب بصريا تلعب دورا أساسيا في زيادة دقة التصنيف الموجه و هذا ينعكس على حساب المنطقة لكل فئة في المشهد. في هذا العمل، ان دقة الكلية قد ازدادة من 68.5٪ إلى 98.9٪ بعد اعتماد تقنية ال(histogram equalization) كتقنية تحسين في تعزيز اختيار منطقة التدريب بصريا.

على الرغم من أن الدقة العالية للتصنيف مع صورة ال(principal component)، ولكن لا تزال عملية التصنيف مع الحزم الأصلي هو أفضل لكون ان قيمها تمثل الانعكاس الحقيقي للطيف. ومما يعزز نتيجة دقة التصنيف مع الحزم الأصلية من 68.5٪ إلى 97.08٪ وأصبحت قابلة للمقارنة جدا مع نتيجة دقة التصنيف مع الصور ال(principal component) 98.86٪ عندما تم تحسين اختيار منطقة التدريب بصريا.

في هذه الأطروحة، تم استخدام برنامج الENVI الإصدار 4.5 لتحقيق الهدف من هذه الدراسة.

جمهورية العراق

وزارة التعليم العالي و البحث العلمي

جامعة النهرين

كلية العلوم

قسم الفيزياء

تصنيف الاداء الموجه و غير الموجه لصور الاقمار الاصطناعية

رسالة

مقدمه الى كلية العلوم / جامعة النهرين

كجزء من متطلبات نيل درجة ماجستير علوم في الفيزياء

من قبل

حسن سالم عبدالمجيد

بكلوريوس/ 2013

بإشراف

الأستاذ دكتور

ليث عبدالعزيز العاني

جمادي الثاني

1437 ه

نيسان

2016 م